NATIONAL AERONAUTICS AND SPACE ADMINISTRATION

Technical Report No. 32-1004

Flow-Visualization Studies of a Confined, Jet-Driven Water Vortex

E. J. Roschke

JET PROPULSION LABORATORY
CALIFORNIA INSTITUTE OF TECHNOLOGY
PASADENA, CALIFORNIA

September 15, 1966

NATIONAL AERONAUTICS AND SPACE ADMINISTRATION

Technical Report No. 32-1004

Flow-Visualization Studies of a Confined, Jet-Driven Water Vortex

E. J. Roschke

Approved by:

D. R. Bartz, Manager
Research and Advanced Concepts Section

JET PROPULSION LABORATORY
CALIFORNIA INSTITUTE OF TECHNOLOGY
PASADENA, CALIFORNIA

September 15, 1966

Prepared Under Contract No. NAS 7-100
National Aeronautics & Space Administration

CONTENTS

TABLES

FIGURES

ABSTRACT

11820

Visual observations, in the form of photographs and sketches, of the flow of water within a confined, jet-driven vortex tube are presented and discussed. This vortex tube had a fixed nominal diameter of 4 in., but was of variable length so that effects produced by changes in aspect ratio could be studied. The basic configuration, having planar endwalls and a single exit hole, was modified by changing the shape of the endwalls and/or installing exit holes at both ends. Conical, hemispherical, and canted endwalls were investigated. The results of other experiments such as injection of a second, heavier-than-water fluid, the insertion of probes into the flow, and the transient effects of changes in mass rate of flow supply are also discussed. It is demonstrated that aspect ratio has a strong influence on the secondary flows in a confined vortex. The principal results are given in the form of color photographs typical of several flow conditions.

Author

I. INTRODUCTION

The flow-visualization results presented here represent a parallel effort to the work reported in Ref. 1; a principal objective of the combined experimental effort was to investigate the effects of aspect ratio on the flow in a confined, jet-driven vortex tube. Aspect ratio is defined as the length-to-diameter ratio L/D. Extensive flow-visualization studies were carried out using a vortex-tube configuration that consisted of a right, circular cylinder having a single, circular exit hole centrally located in one endwall. Water was the motive fluid and visualization was accomplished by observing the motions of various colored dyes both visually and by means of still and motion picture photography. Changes in aspect ratio L/D, relative exit-hole size d_e/D, and mass rate of flow $\dot{m}$ were studied in this configuration. Other cylindrical vortex-tube configurations having exit holes at both ends rather than a single exit hole at one end, or having non-planar endwalls, were also investigated. In addition, effects on the vortex flow produced by probe insertion, injection of a liquid heavier than water (carbon tetrachloride), and time variations in the flow supply were observed. These experiments were in many respects very similar to the work of Ross et al. (Ref. 2 and 3) except that their apparatus employed a fixed aspect ratio and

considerably smaller mass flow rates. Their observations of secondary-flow structure in vortex tubes and those reported here are in substantial agreement.

Extensive use of flow visualization as a tool for studying rotating flows is probably due to the fact that it provides a rapid and economical method of studying secondary-flow structures, which are not always readily detected by probes. Probings of vortex flows are very difficult and subject to much uncertainty, so that the use of flow visualization, despite many limitations, may be readily appreciated. Dyes have been commonly exploited as trace fluids in rotating water flows (Ref. 2–8) and smoke has been similarly used in gas flows (Ref. 9–11). Two novel and interesting techniques for visualization in water flows are presented in Ref. 12 and 13, which are concerned with flow between concentric rotating cylinders and flow about a rotating sphere, respectively. However, those methods are not likely to be useful for visualizing confined vortex flows except, perhaps, for visualizing cross sections of the flow in the plane of rotation, i.e., end views. The use of neutrally buoyant particles (Ref. 14) has been proposed as a method for obtaining quantitative data in vortex flows (Ref. 15); however, great care must be exercised in the interpretation of such data when applied to rotating flows. A variation of this technique was successfully applied some years ago to determine the velocity components in a hydraulic cyclone (Ref. 16).

The experimental study of the effect of nonplanar endwalls in rotating flows has intrinsic interest from a fluid-mechanics standpoint, as well as practical interest in that conical endwalls, for example, are commonly used in cyclone separators and swirl atomizers. Both interests stimulated the work herein. It was, perhaps, the successful use of conical endwalls in cyclone separators that prompted an adoption of such walls in the vortex configuration suggested in Ref. 17. Observations in configurations with canted endwalls were performed as an extreme test case with application to the possible effects produced by small, unintentional irregularities of this type in configurations with otherwise planar endwalls. The hope was that flow-visualization studies in the various vortex configurations would reveal at least the gross features of the secondary-flow structure and in what ways these features might differ from those observed in more conventional configurations.

The principal results offered here are given in the form of color photographs typical of several flow conditions. Extensive motion pictures were taken, although no reference can be cited for these at the present time.

II. DESCRIPTION OF APPARATUS

A schematic view of the vortex tube and its principal dimensions is shown in Fig. 1. A vortex, driven by two rows of tangentially oriented jets, was generated within a right, circular Plexiglas cylinder that had a single, circular exit orifice located centrally in one endwall. The endwall containing the exit hole was movable in the axial direction so that the vortex aspect ratio was variable in the range $0 < L/D < 12$. A more detailed description of the vortex tube and its attendant flow system is given in Ref. 1 and will not be repeated here. The closed endwall and one or both of the apparatus sidewalls (Fig. 2) were fabricated from transparent Plexiglas so that dye motions within the vortex could be observed from either direction merely by relocating the light source. Distortion produced by a direction of view normal to the cylindrical surface of the vortex tube was reduced by immersing the tube in water as indicated in Fig. 2. This technique was utilized in Ref. 16 and is discussed briefly in Ref. 18. The vortex-tube configuration shown in Fig. 1, which hereafter will be referred to as "standard configuration," could be modified by (1) replacing the piston assembly to obtain different exit-hole sizes, (2) replacing the piston assembly and closed endwall with combinations of nonplanar shapes, and (3) by replacing the closed endwall with one having an exit hole, thus providing double-exit-hole configurations.

A series of dye-injection ports (Fig. 3) distributed at approximately 4-in. intervals in the axial direction along both the top and bottom of the vortex tube permitted radial injection of dye. Each of these ports was provided with a sliding, hollow probe or tube that could be retracted flush with the cylindrical wall or inserted to any

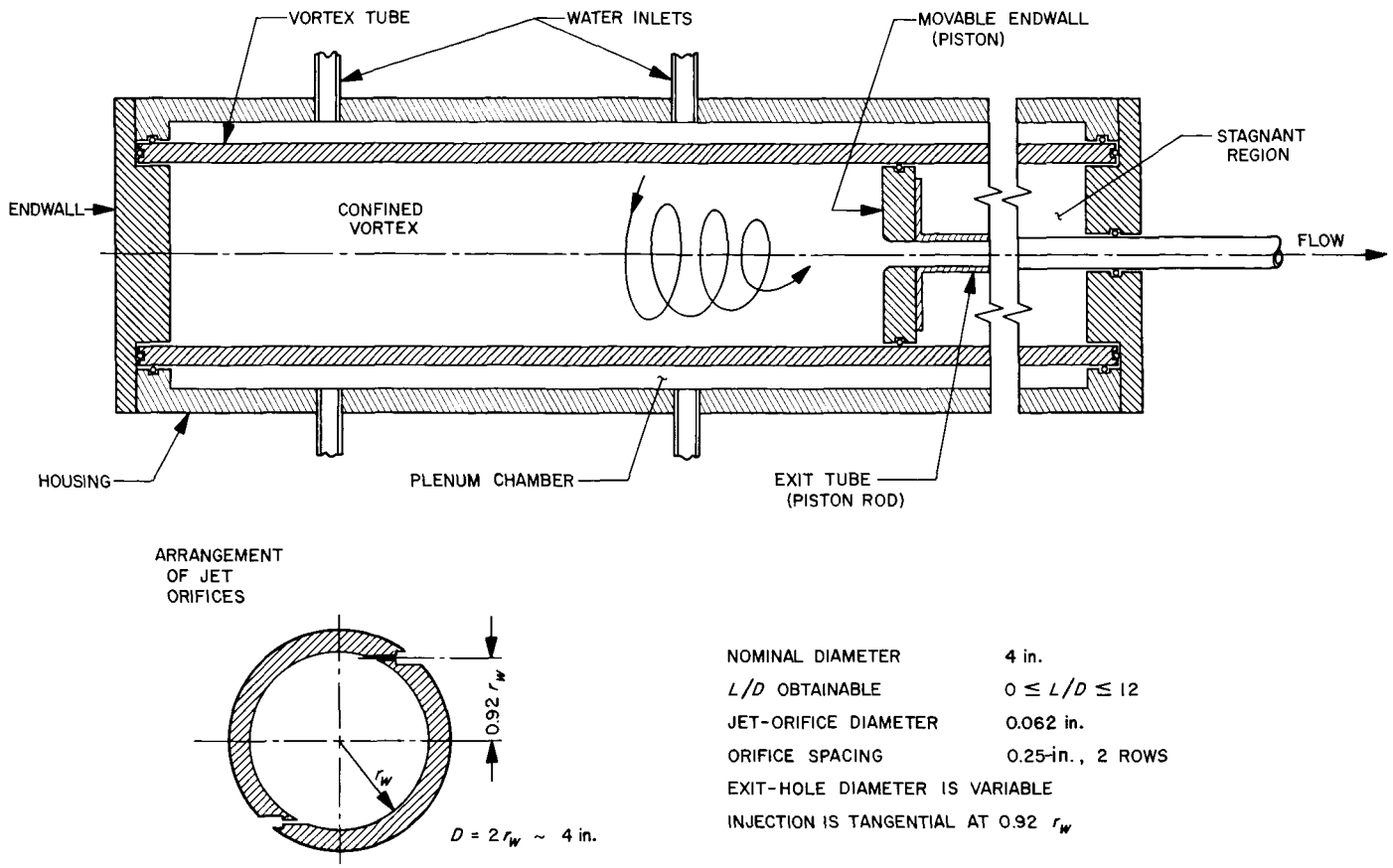

Fig. 1. Schematic arrangement of 4-in.-diam. water-vortex tube

desired radial depth into the vortex flow. Another system of small tubes was positioned in the plenum chamber and designed to release dye in close proximity to a selected number of driving-jet orifices, thus providing tangential dye injection. The spacing of the latter injection sites coincided approximately with the ports first described. A third method of dye injection sometimes used was injection through static-pressure taps located in the closed endwall.

Two water-soluble dyes, which are actively fluorescent under long-wave ultraviolet illumination, were used extensively: dichlorofluorescein and rhodamine B. Under illumination, these dyes appear green to yellow and orange to yellow, respectively, depending on their concentration and the intensity of illumination. Concentrated dye solutions, premixed from small amounts of powder dissolved in ordinary water, were stored in separate, nitrogen-pressurized tanks. Each dye-supply line contained a manual, on-off-type toggle valve so that dye could be released at any time and at any of the injection sites desired. Further discussion of dye selection is given in the Appendix.

Initially it was intended to use ultraviolet light for illumination. When it was discovered that "white light" produced colors, brilliance, and contrast not greatly different than ultraviolet, the latter was discontinued in favor of a commercial 1000-watt Sun-Gun employing a mercury-vapor lamp; however, greater intensities were required. Using white light also simplified both visual and photographic observation. The light source, indicated schematically in Fig. 4 by a light bulb, was housed within a blackened, air-cooled tube, which in turn was mounted on a portable stand. A sheet of infrared reflecting glass was inserted between the light source and the Plexiglas endwall or sidewall of the vortex-tube housing to minimize heat-transfer effects.

The general lighting arrangement indicated in Fig. 4 was the one most often used. In Fig. 2, the direction of the light would be through the transparent, closed endwall (not shown) into the plane of the figure. Because of the schematic nature of Fig. 4, only one row of tangential driving jets is indicated, rather than two, and the sense is opposite to that actually used (Fig. 2) so as not to obscure the drawing. With this arrangement one observes

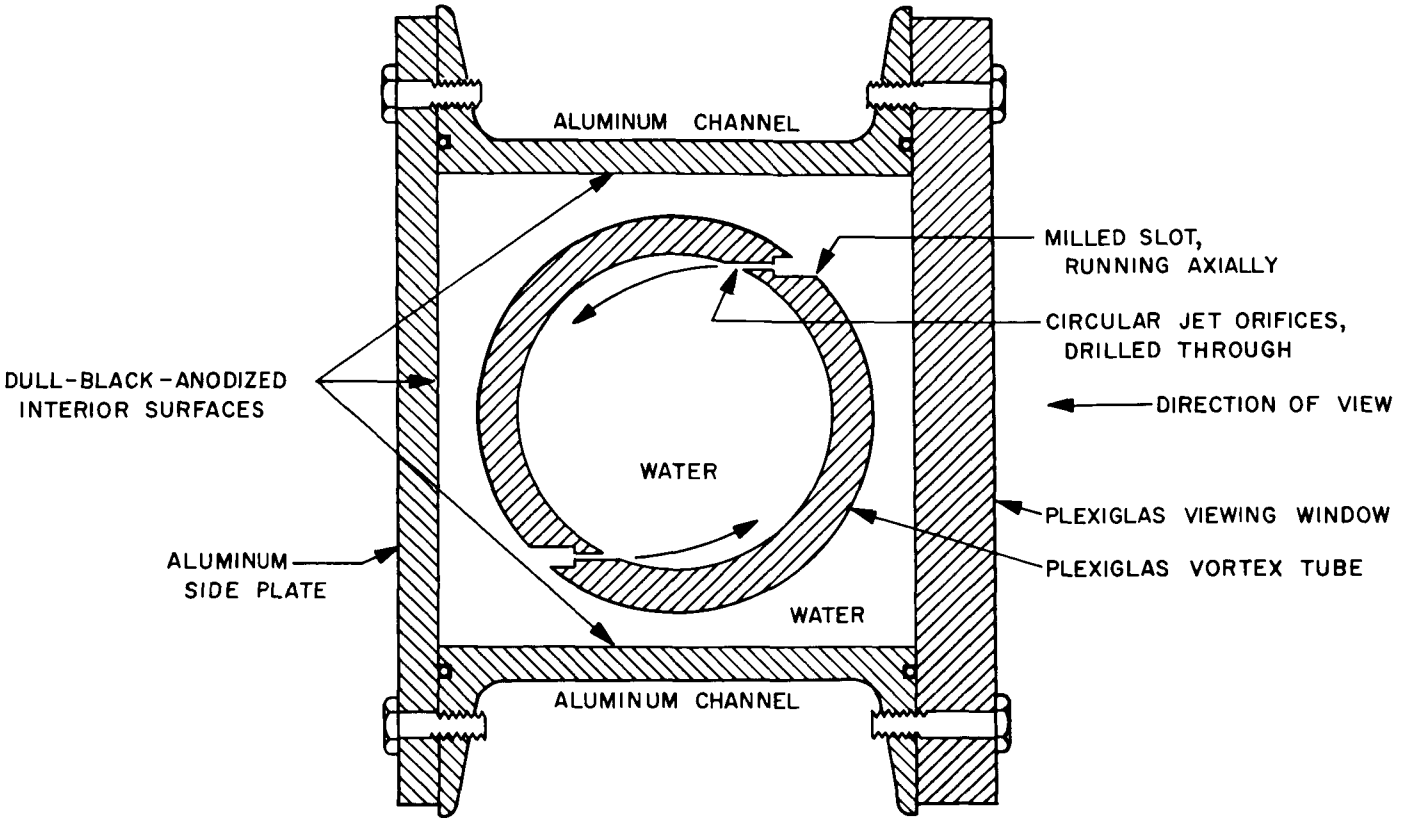

Fig. 2. Cross section of vortex apparatus as viewed from direction of closed endwall, *showing arrangement for flow visualization*

primarily the axial, but also the radial, flow components. When end views were desired, the positions of lighting and sighting were interchanged and one could observe tangential motions by sighting through the closed, transparent endwall. In the latter case, as will be shown later, a shadow caused by the milled slot in which the driving-jet orifices were located (Fig. 2) was particularly evident.

Flow-visualization studies were undertaken in a darkened room and, to enhance the color contrast of the dyes as much as possible, all interior surfaces of the vortex-tube housing were given a dull-black finish, as shown in Fig. 2. Even so, light reflections from the inner curved surface of the vortex tube tended to inhibit color contrast and sharpness, but were reduced by another means to be discussed presently. The best possible background for observation would have been a dull-black coating on the rear half of the interior vortex-tube surface, as viewed according to Fig. 2 and 4; however, this was not feasible because variations in L/D or piston movement were required. Instead, light was passed through a vertically oriented slit, through the transparent endwall, in the direction of the opposite endwall containing the exit hole (Fig. 4). This arrangement had the dual advantage of markedly reducing internal reflections because the walls were not directly illuminated, and providing means for studying cross sections of the flow. Slit widths of 1/16 to 1/2 in. were used; a width of 1/4 in. was considered best, overall, for this apparatus. Considerable time was spent in an attempt to improve the sharpness and collimation of the light sheet (produced by the slit) by means of various optical systems. This was difficult because the optical path length in the water, which sometimes contained large amounts of dirt and/or gas in solution, varied from several inches to 4 ft.

These attempts were abandoned because (1) the optics reduced the intensity of illumination to an unacceptable level and (2) the presence of dirt and minute gas bubbles in the water, which varied from day to day, introduced absorption and scattering of light, thus precluding successful use of an optics system. As a result, the divergence of the light sheet became noticeable for $L/D > 2$ and rather extreme for $L/D > 6$.

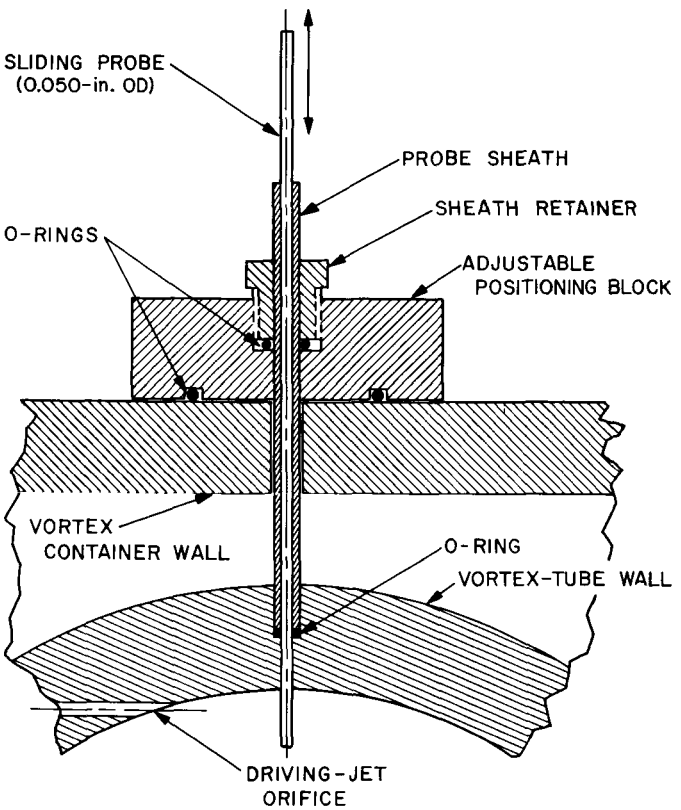

Fig. 3. Port arrangement for insertion of probes into vortex tube

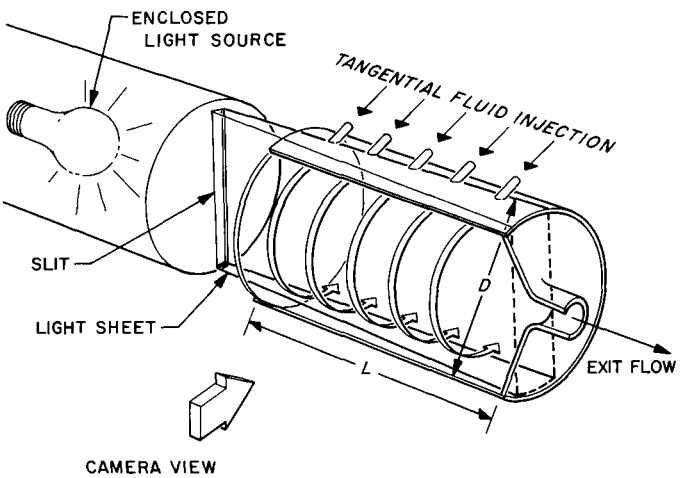

Fig. 4. Schematic arrangement for vortex visualization (shown for only one row of injection orifices, with direction of injection opposite to that actually used)

Nevertheless, use of a light sheet proved superior to the use of a beam of circular cross section. Not only were internal light reflections from curved surfaces decreased, but the reduced field of view tended to permit a more detailed examination of secondary-flow structure. The use of two dyes of different color was advantageous, since relative fluid motions occurring in very thin or narrow regions were more readily detected. Aside from still photographs most often taken with an exposure time of $\frac{1}{25}$ sec, extensive motion picture coverage at 24 frames/sec was provided. A limited amount of footage was also taken at film speeds of 64 and 128 frames/sec. Comments on color film used are given in the Appendix.

III. EXPERIMENTAL PROCEDURE

A. Conditions of Visualization

The visualization procedure employed was simple, with little technique other than assuring proper timing of dye injections. This was more important for still picture photography than motion picture photography. After first selecting the configuration to be studied and positioning the light source and camera, the desired flow conditions such as aspect ratio L/D and either static pressure at the cylindrical wall p_w or mass rate of flow $\dot{m}$ were arranged. Means for setting flow conditions, daily water conditions, and various difficulties in operating the apparatus are discussed in Ref. 1. Color dyes were injected at the desired locations and their subsequent motions were either observed visually or photographically recorded. Dye was sometimes injected from several sites simultaneously and at other times sequential injections were used. The amount of dye injected depended, of course, on the pressure used in the dye reservoirs relative to the environmental pressure existing at the injection site, as well as upon the duration of injection. The injection pressure was regulated and continuously variable. Large injection pressures (or more properly, injection-pressure differences) resulted in the ability to inject large amounts of dye in relatively short

intervals of time, but this technique also produced noticeable flow perturbations. Smaller injection pressures required longer-duration injections, but did not disturb the vortex flow as much. Some compromise was selected so as to be appropriate to each test condition. Dye-reservoir pressures exceeding the static wall pressures in the vortex by approximately 5 psi were normally used.

B. Configurations Investigated

The various vortex configurations investigated are shown in Fig. 5; information concerning exit-hole size and type of observation for each of the configurations is given in Table 1. These configurations fall into three categories: (1) conventional configurations with single or double exit holes, (2) configurations with nonplanar endwalls, and (3) configurations with submerged exit tubes, single or double exits. The aspect ratio L/D of these configurations is based on the exposed length of the cylindrical wall; i.e., that portion of the vortex tube exposed to tangential driving-jets. The single exception is configuration J, with canted and opposed endwalls, for which an average length is appropriate. In all configurations, long exit tubes (a minimum of 72 pipe diameters) were used to convey water from the vortex tube to atmospheric conditions; these exit tubes also served as piston rods (Fig. 1). Reference 1 contains discussion pertinent to these exit tubes.

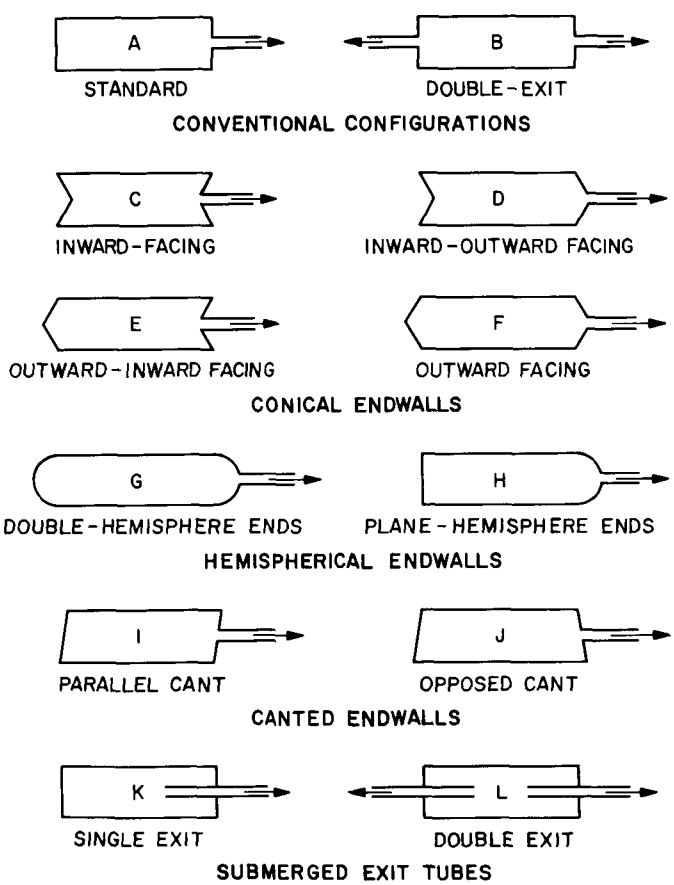

Fig. 5. Vortex-tube configurations examined by flow visualization; all conical surfaces had 120-deg vertex angles; canted surfaces had 10-deg cant; aspect ratio variable in all cases

As might be expected, the use of nonplanar endwalls produced some rather pronounced distortions when slit illumination was introduced through these endwalls. In some cases the illumination was rather poor, especially at large values of L/D. Because of difficulty in positioning, illumination of vortex flows having double exit holes (and exit tubes) was not very satisfactory in this particular apparatus.

C. Effects of Dye Injection

The effects on foreign substances placed in rotating flows may be significant if the foreign material possesses a specific gravity much different from that of the carrier fluid. Very small differences in specific gravity become apparent in a strong centrifugal field; the performance of centrifuges and ultracentrifuges is based on this principle. Therefore, some care must be exercised when interpreting motions of trace fluids; e.g., dyes used for flow visualization. Reference 2 contains a discussion of specific-gravity balancing as applied to the use of light-absorbent-type dyes (methyl violet, nigrosine black, etc.) in water-vortex flows. Fluorescent-type dyes generally may be used at lower concentration levels than light-absorbent-type dyes. In the present experiments, hydrometer readings for determining specific gravity of dye solutions were not taken, partly because no special recipe for mixing the solutions was used. Since the dyes used were completely water soluble, the solutions thus formed were of colloidal nature. Separate experiments were performed in an attempt to estimate the effects of gravity and laminar, concentration-gradient diffusion on droplets of dye carefully placed in containers of still, clean water. Both effects were found to be minimal under those conditions. Individual filaments of dye remained visible to the eye for periods of time exceeding a half-hour in natural light and could still be detected hours later under long-wave ultraviolet light. However, it should be pointed out that maximum radial accelerations in the vortex experiments approached values 5000 times greater than gravitational acceleration. In Ref. 7 it was reported that attempts to centrifuge fluorescein dye solutions were unsuccessful, which shows that fluorescein is completely soluble in water.

Table 1. Flow-visualization experiments in the 4-in.-diam. water vortex with variable aspect ratio

Configuration	Nominal exit-hole diameter d_e, in.[b]	Observations			Principal visual features
		Visual	Still pictures[c]	Motion pictures[d]	
A[a] (standard)	3/8	✓		✓	Secondary-flow patterns strongly dependent on aspect ratio, but not mass rate of flow, at low L/D. Patterns more dependent on $\dot{m}$ at high L/D.
	1/2	✓	✓	✓	
	5/16	✓	✓	✓	
	1	✓		✓	
B	3/8	✓		✓	Unsymmetric secondary flow patterns
C	1/2	✓		✓	Strong axial and radial flows
D		✓		✓	Complex but well defined secondary flows
E		✓		✓	Pronounced radial outflow near endwalls
F		✓		✓	Secondary-flow patterns diffuse, not well-defined
G		✓		✓	Flow very unsteady; whirling-core flow
H		✓		✓	Flow somewhat unsteady; patterns similar to C
I		✓		✓	Sinuous, undulating-core flow
J		✓		✓	Sinuous-core flow; unsteady
K	3/8	✓		✓	Turbulent, separated corner flow
L		✓		✓	Separated corner flow; unsymmetric patterns

[a] Quantitative data contained in Ref. 1.

[b] Configurations A, B, K, and L had exit holes with inlet edges rounded to 1/4-in. radii. All others had sharp-edged exit holes.

[c] At exposure times of 1/50th to 1/25th sec.

[d] At frame speed of 24/sec; some sequences at 64 and 128 frames/sec.

Another matter of interest is the perturbation effect upon the local flow within a vortex tube due to an injection of dye. Such effects can be discussed only qualitatively, because the amount of excess momentum possessed by a burst of fluid dye, over and above the local flow, was highly variable. In the case of radial injection the dye would, of course, also have a radial component of velocity, so that disturbances produced by this type of dye injection would be greater than for tangential injection. Figure 6 shows photographs of both types of dye injection in the standard configuration, as viewed through the closed endwall. The photographs represent a cross section of the flow under illumination through a ¼-in. slit located at $L/D=2$ from the closed endwall and at the right-hand side of the vortex tube, which is oriented as shown in Fig. 2. Dye was released within the light sheet (at $L/D=2$) through a port in the top for radial injection, but through a lower driving-jet orifice for tangential injection. The flattened portions seen at the top of each photograph are shadows caused by the milled slot (Fig. 2). During injection, the flow patterns produced by the different methods of dye injection were decidedly different. However, at a later time, after the dye had been shut off and the residual allowed to spiral inwards, the patterns would appear very similar. Further comments on these photographs will be given later. Side-view observations of the vortex flow during strong and prolonged radial injections of dye revealed that transient, fast-moving axial counterflows could be generated in this way. These counterflows were usually, but not always, unsteady, and very quickly ceased upon termination of injection. Tangential injections of dye did not appear to disturb the flow significantly.

Dye injection into the endwall boundary layers produced different effects, depending on whether or not the

dye penetrated through the boundary layer. Dye injected so as to barely seep out of an endwall pressure tap apparently remained within the boundary layer, moved rapidly inward radially, and was discharged into the main stream at or near the center (in the case of the closed endwall). Dye contained in fluid layers more distantly removed from the endwall generally erupted from the vicinity of the endwall earlier, i.e., at larger radii. By carefully varying the degree of pressurization on the dye-supply tanks and observing the results of equally careful injection in or near the endwall, one could obtain a crude, qualitative idea of the relation between tangential and radial velocity components in the endwall boundary layer. These motions were not successfully photographed because the dye concentrations were generally too low and the contrast poor. Unfortunately, because of the construction of the vortex tube, similar observations at the exit-hole end of the vortex were not possible.

IV. EXPERIMENTAL RESULTS

Results for configuration A, the standard configuration shown in Fig. 5, are presented in the form of color photographs (Fig. 6–12) to indicate some of the effects of aspect ratio L/D and static pressure at the cylindrical wall p_w (or alternatively the mass rate of flow $\dot{m}$) on the confined water vortex. The visual effects produced by the insertion of probes into the flow are illustrated in Fig. 11 and 12. These results are expanded by comments made on the basis of visual observations and results recorded by motion picture photography. Since still photographs were taken of the standard configuration only, verbal descriptions of flows in other configurations are given. However, an attempt has been made to illustrate the more singular features of flows in the remaining vortex configurations by means of freehand sketches.

With the exception of Fig. 6, all flow-visualization studies are side views made in the manner indicated in Fig. 4. The closed endwall is to the left-hand side of each photograph. Fluid was injected tangentially through the rows of orifices, which appear as small, pale circular spots at the top and bottom of the illuminated area. These views do not show the tangential velocity component, which has a direction into the plane of the paper at the top of the photographs and conversely at the bottom of the photographs. Illumination was introduced through the transparent, closed endwall by means of a ¼-in.-wide, vertically oriented slit. The axial positions of dye-injection sites are indicated in Fig. 7–12. In these photographs green dye was introduced tangentially, whereas the yellow dye was introduced radially. Small, black arrows have been superimposed on the photographs to indicate the direction of the more clearly defined axial flows and counterflows (secondary flows). In the end-view studies shown in Fig. 6, the direction of fluid motion is counterclockwise; direction of dye injection is indicated.

All but one of the photographs were taken using an exposure of 1/25 sec and therefore they represent results over this small time increment, which was part of a much longer duration dye transient. They were not taken at precisely the same time relative to the initial dye injection, nor was the dye injected in precisely the same way or at the same locations each time. Sometimes dye photographs made under the same experimental conditions appear somewhat different because the dye motions are in a different stage of development and the dye locations within the vortex differ. Motion pictures are much more instructive for these reasons. The photographs were all taken under conditions of "steady" flow; i.e., with all controllable experimental conditions held fixed. However, the term steady flow is often used rather loosely and tends to be used to describe degree. The vortex flow was never precisely steady in the technical sense and was often decidedly nonsteady; discussions concerning steadiness are contained in Ref. 1. Visual and photographic observations indicated that the large majority of secondary flows rendered visible by dye motions were reproducible. In a small number of cases this was not true for reasons that were never ascertained.

A. Conventional Configurations

1. Standard Configuration

Flow-visualization studies in the standard configuration A (Fig. 5) indicated that secondary-flow structure was largely controlled by the aspect ratio when $L/D < 4$, whereas the effects of p_w or mass rate of flow $\dot{m}$ became increasingly more evident at larger values of L/D. For $L/D > 6$, increasing values of aspect ratio did not appear to produce significant changes in secondary-flow patterns. In Ref. 1 it was reported that air-core diameters in the water vortex depended strongly on relative exit-hole size d_e/D and aspect ratio L/D, but were not markedly influenced by pressure or mass rate of flow.

Figure 7 clearly indicates the strong influence of aspect ratio on secondary-flow patterns at lower values of L/D; in this series of photographs the exit-hole diameter and the static wall pressure are fixed (except for the case of $L/D = 3$). Note that the air core, which appears as a rod aligned with the vortex axis, diminishes in diameter with increasing L/D. Alternate injections of either color of dye were used to make visible the complex interlacing of axial flows and counterflows at $L/D = 1$ and 1.5. Dye fronts assumed the shape of hollow bodies of revolution, which were, however, not strictly cylindrical. At $L/D = 1$, fluid discharge from the endwall boundary layers occurred over a large portion of the endwall area; the boundary layers at the two endwalls appeared to exchange fluid several times before the fluid passed through the vortex. It appeared that eight axial-flow reversals occurred at $L/D = 1$ and five reversals occurred at $L/D = 1.5$. In both cases a region of near-zero axial flow existed; dye appeared to diffuse slowly into this region, but remained significantly longer than at any other location. The flow at $L/D = 1$ was strongly stratified in the radial direction and appeared to be laminar regardless of the mass rate of flow; at $L/D = 1.5$ the flow was less strongly stratified and appeared turbulent near the cylindrical wall. At values of $L/D > 1.5$ the flow took on a somewhat different aspect, appearing more and more like a bathtub vortex. The strong central jet originating at the closed endwall, and passing axially from left to right in the photographs, diminished markedly in diameter and the axial-counterflow region originating at the opposite endwall became thickened in the radial direction. Discharge from the endwall boundary layers appeared to be confined to smaller regions near the center of the vortex. Flow in the outer annular region, i.e., outside of the region of strong axial flow, appeared turbulent. The overall effect of increasing L/D thus seems to be a relative decrease in influence of the endwall boundary layers. The secondary-flow structure at $L/D = 3$ (Fig. 7) appears very similar to diagrams presented in Ref. 2 and 3.

The effect of increasing mass rate of flow $\dot{m}$ is shown in Fig. 8 at fixed $L/D = 1.5$. Mass rates of flow are approximately in the ratio $1 : \sqrt{2.5} : \sqrt{10}$ in this series of photographs, corresponding to values of $p_w - p_a$ of 2, 5, and 20 psig, respectively. Note that the diameter of the air core and the central jet does not change with increasing $\dot{m}$. Except for differences in the shape of dye fronts originating at the closed endwall, the only apparent difference in this series of photographs is the relative sharpness and/or diffuseness of the dye interfaces. As $\dot{m}$ increases, fluid velocity also increases, which leads to more rapid mixing of dye; the finer details of individual dye filaments become smeared out. The gray areas located between the inner green cylinder and the outer orange annulus do not represent dye, but rather indicate gas coming out of solution from the water, forming minute bubbles that move radially inward to form the core. As discussed in Ref. 1, air cores were formed by this process in this apparatus and not by entry of atmospheric air into the subatmospheric pressure regions near the vortex axis.

Figure 9 contains a series of photographs much like those shown in Fig. 8, except that the exit hole is slightly larger and $L/D = 5.33$. Again, the dye patterns appear more diffuse as $\dot{m}$ increases. An axial counterflow is clearly evident in each photograph; its radial thickness decreased with increasing $\dot{m}$. The only other detectable axial flow counter to the direction of the central jet was a very weak axial flow from right to left in an annular region adjacent to the cylindrical wall. That flow existed in a region extending from the closed endwall to an axial location perhaps 3 to 4 L/D from the closed endwall, beyond which an axial flow was directed toward the opposite endwall.

A series of photographs showing dye studies in proximity to the closed endwall (when the vortex was set at $L/D = 6$) is shown in Fig. 10. The first two photographs, both at $p_w - p_a = 5$ psig, were taken at different stages of dye-motion development after a single color of dye was injected at $L/D = 1$ from the closed endwall. The first photograph shows the development of a typical conically shaped counterflow region taken just at time of arrival of the dye at the closed endwall. It is of interest because it shows radial outflow occurring outside the endwall boundary layer, a phenomenon probably not caused by diffusion. It appeared that fluid from the counterflow region split into two portions; some was entrained by the

endwall boundary layer, subsequently to be discharged into the central jet, and some first flowed radially outward before becoming entrained in the endwall boundary layer. References 2 and 3 show diagrams of flow from the counterflow region entering a concentric axial-flow region surrounding the counterflow region. In the present study, a separate experiment was arranged to investigate this phenomenon. A small hollow tube, coincident with the vortex axis, was inserted through the closed endwall so that it could be moved axially to any desired depth along the vortex axis. Near the closed endwall, some of the dye injected through this small tube was observed to move radially outward. When some critical immersion depth had been exceeded, i.e., the axial position of the tip of the tube measured from the endwall, radial outflow ceased and only axial motion was visible.

Close observation of the interaction between the axial counterflow and the boundary layer on the closed endwall revealed that the process was generally not steady. An oscillating motion between predominantly radial outflow, then predominantly radial inflow, seemed to occur. The second photograph presented in Fig. 10 shows green dye in a later stage of development compared to the first photograph. It is suggested that the camera "stopped" the motion of the dye shortly after an oscillation from radially outward flow to radially inward flow occurred. Note the peculiar lyre-shaped region that contained no dye.

The third photograph presented in Fig. 10 shows yellow dye, which had been injected near the closed endwall, discharging into the familiar center jet and also forming a concentric axial-flow region surrounding the center jet. The thin, clear region between them was occupied by an axial counterflow. Compare this photograph with those shown in Fig. 9. At larger values of L/D the annular region of flow external to the central region of high axial velocity invariably appeared to be turbulent.

End views of the vortex flow corresponding to that shown in Fig. 10 have already been discussed in reference to Fig. 6. In Fig. 6 illumination was arranged so that dye motions injected at $L/D = 2$ from the closed endwall could be observed through that endwall. When observing the transient dye motion in this way, one received the impression of concentric rings of dye, each of successively smaller diameter, forming with the passage of time. Some of these rings had sharply defined boundaries and others did not. A much more striking display of this phenomenon was arranged by setting $L/D = 1$ and illuminating the vortex cross section by means of a slit placed at $L/D = 0.5$. The many axial flow regions that occurred in that case (Fig. 7) were successively revealed as the dye moved radially inward via the endwall boundary layers.

2. Probe Effects

One of the purposes of visualization studies with probes placed in the vortex was to investigate the effects of probes of the type used by Pivirotto (Ref. 19). These probes consisted of very small hollow tubes stretched, under tension, across a diameter of the vortex tube. References 1 and 19 contain quantitative data indicating the degradation imposed on a vortex flow by probes of this type. The visualization results are presented here in Fig. 11. An experiment was performed in the water vortex so as to duplicate the gas-vortex configuration used by Pivirotto as nearly as possible, using wires to simulate probes. These conditions required $L/D = 5.33$ and $d_e/D \sim 0.14$. Visualization results for various wire sizes are shown in Fig. 11, which includes a result with no probe for comparison. All photographs were obtained with $p_w - p_a = 5$ psig. Note that the first photograph (no probe) was taken under the same conditions as the center photograph in Fig. 9. Because of light reflection and scattering, the diameters of the probe wires in Fig. 11 appear larger than their actual size.

It is apparent that the presence of these probe wires greatly disrupts the vortex-core flow and has the effect of enlarging the size of the center jet in some proportion to the wire diameter. It was determined that the larger the wire the more effective it became in preventing axial flows across the plane of its location. This was due, no doubt, to the relatively larger radial inflows existing in the wake of the probe as compared to other locations in the vortex. Thus, probe wires produce an effect similar to that of a closed endwall except to a lesser degree. Dye injected in either region between a probe wire and an endwall tended to remain there except near the center of the vortex. It also appeared that the presence of a probe wire caused an additional pair of concentric, axial-flow and counterflow regions to occur in the portion of the vortex between the closed endwall and the plane of the probe. Quantitative results indicated that even very small probe wires produced a measurable degradation in vortex strength.

Some results obtained for cylindrical probes, cantilever-mounted, are shown in Fig. 12; the probe used was 0.050 in. in diameter. Both photographs in Fig. 12 were taken as different color dyes were simultaneously injected near the closed endwall and from the tip of the probe. In the first photograph the probe had been inserted near the vortex-core region; dye issuing from the probe tip

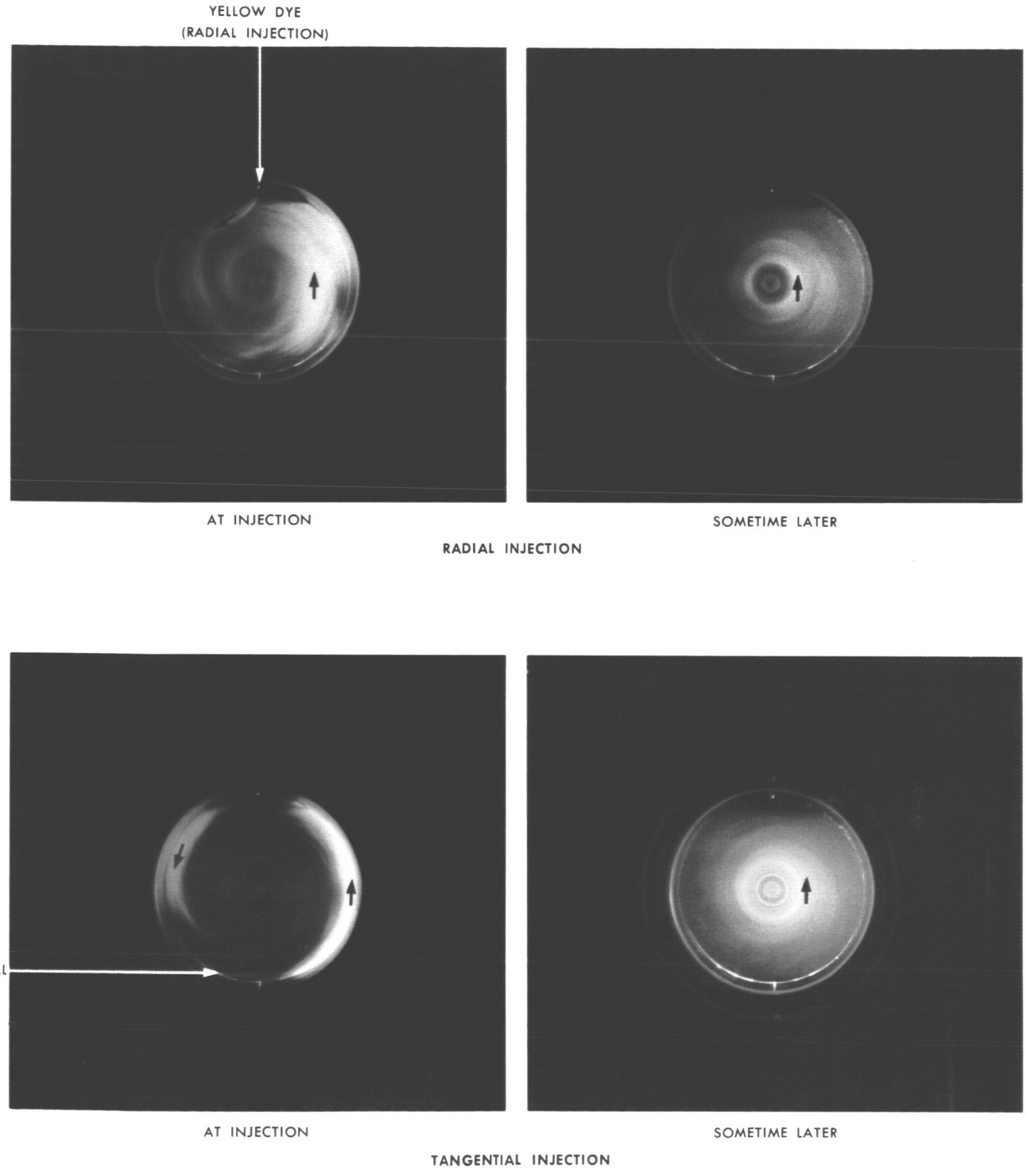

Fig. 6. End views of standard configuration with nominal ½-in. exit hole; $L/D = 6$; $p_w - p_a = 5$ psig; illumination through ¼-in. slit at $L/D = 2$; dye released at $L/D = 2$

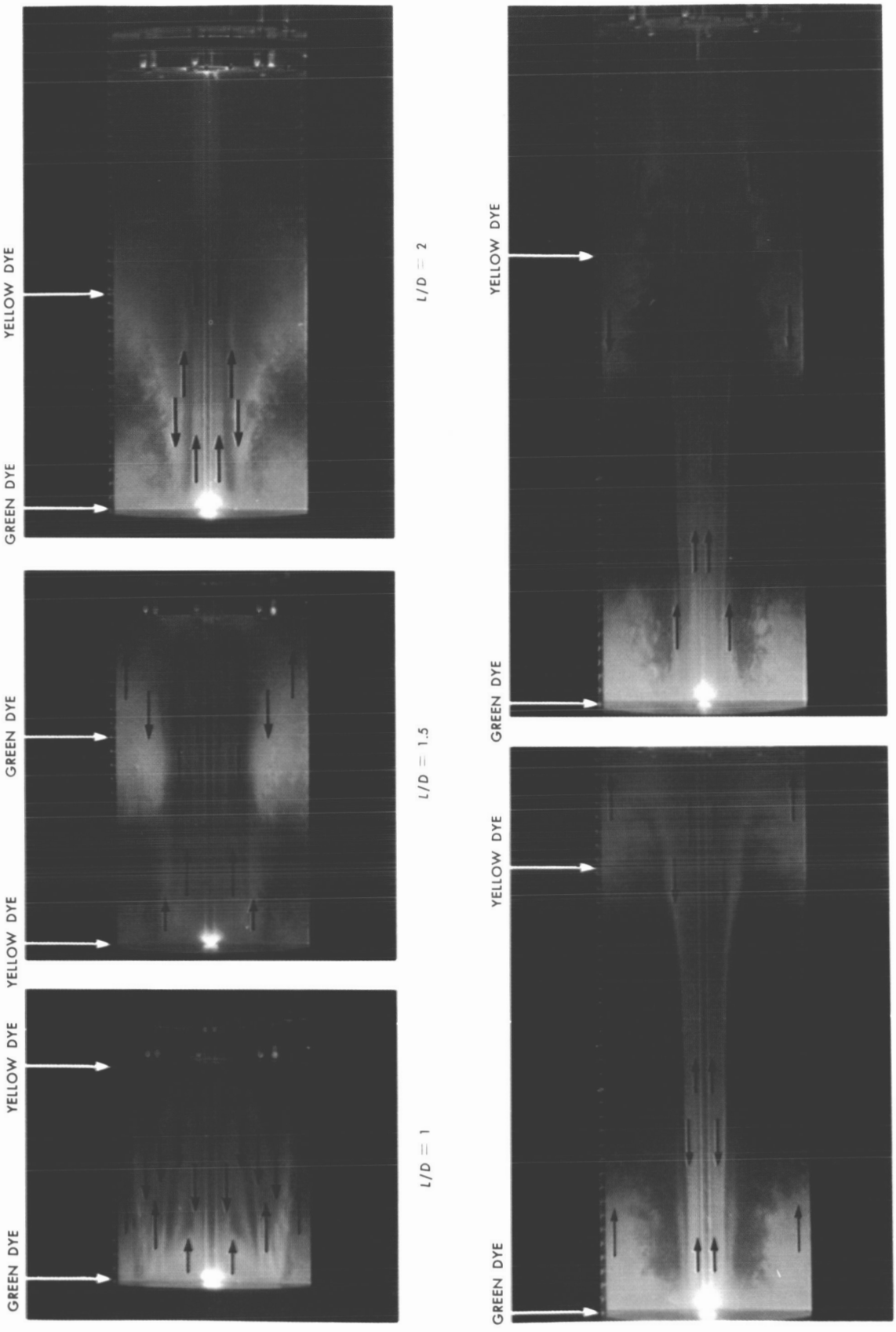

Fig. 7. Dye studies in standard configuration: Effect of aspect ratio at low values of L/D and $p_w - p_a = 5$ psig with nominal ½-in. exit hole (at $L/D = 3$, $p_w - p_a = 2$ psig)

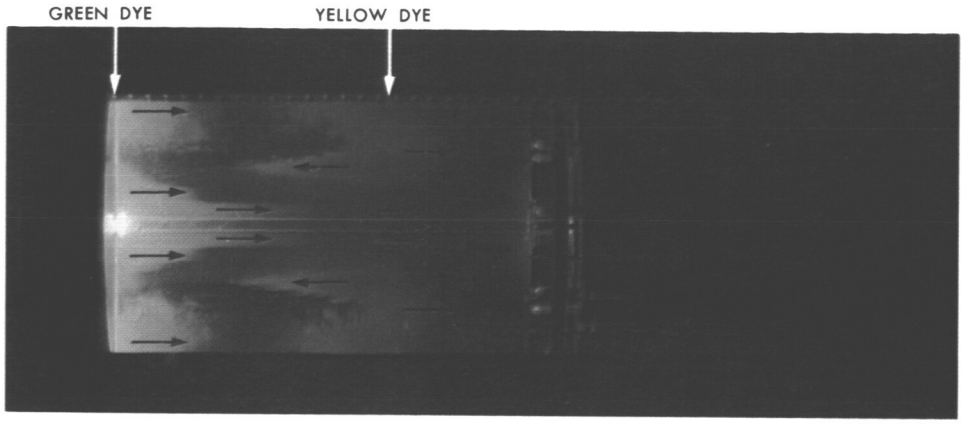

$p_w - p_a = 2$ psig

$p_w - p_a = 5$ psig

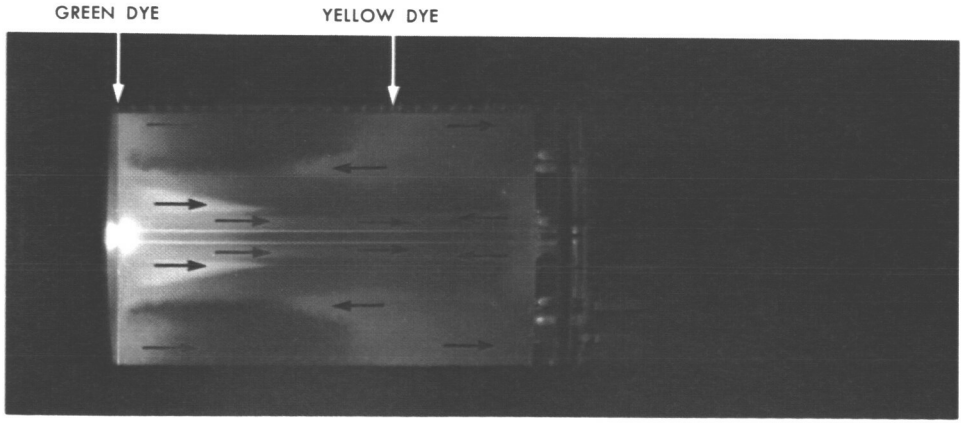

$p_w - p_a = 20$ psig

Fig. 8. Dye studies in standard configuration: Effect of static wall pressure at $L/D = 1.5$ with nominal ½-in. exit hole

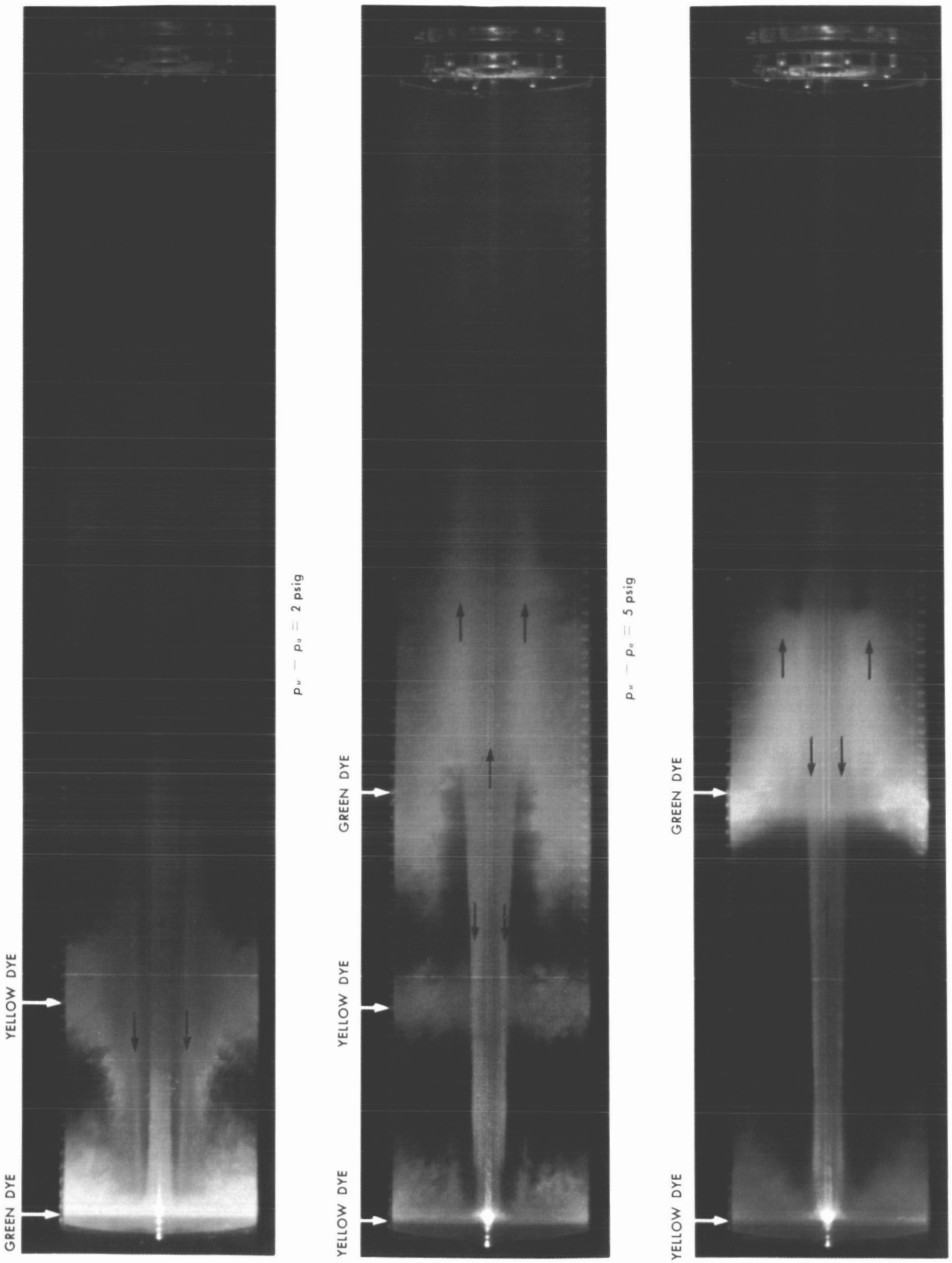

Fig. 9. Dye studies in standard configuration: Effect of static wall pressure at $L/D = 5.33$ with nominal 9/16-in. exit hole

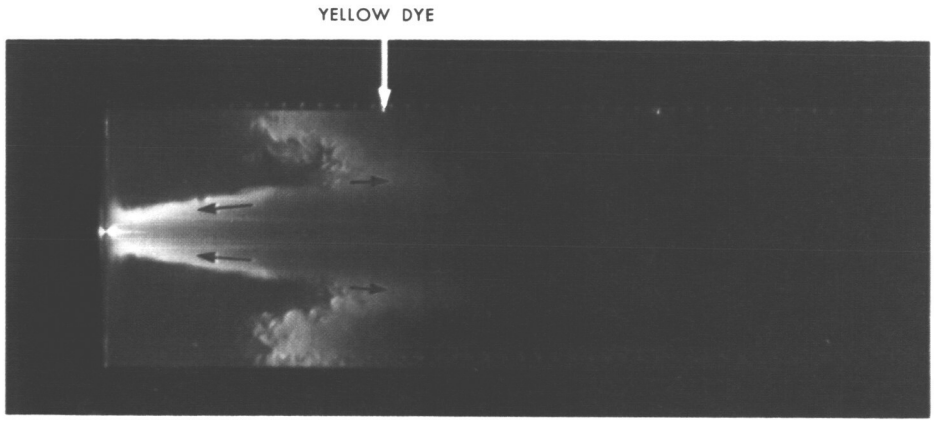

$p_w - p_a = 5$ psig

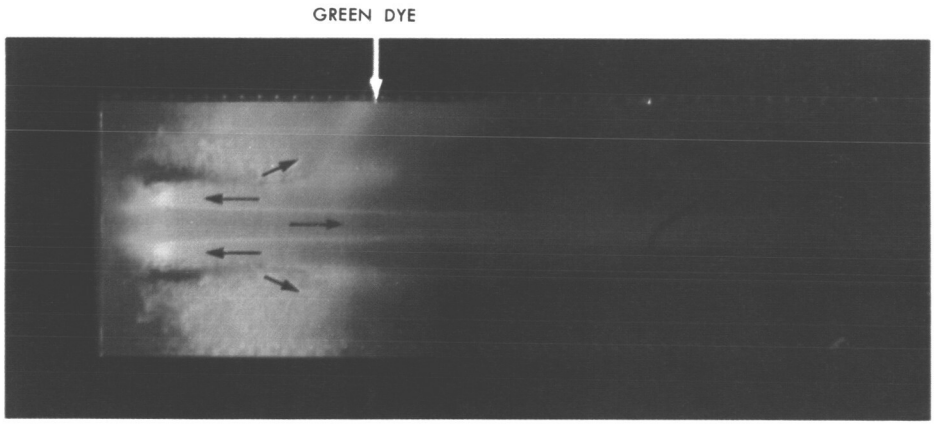

$p_w - p_a = 5$ psig

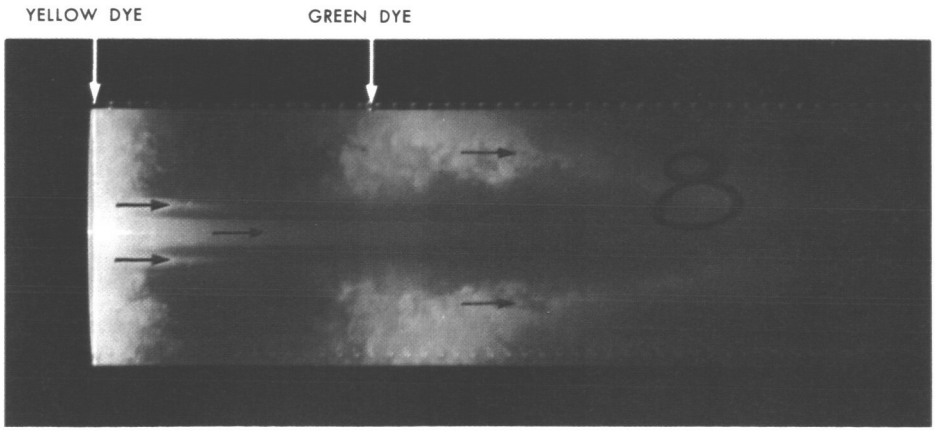

$p_w - p_a = 20$ psig

Fig. 10. Dye studies in standard configuration: Views of a portion of the vortex near the closed endwall, at $L/D = 6$ with nominal ½-in. exit hole

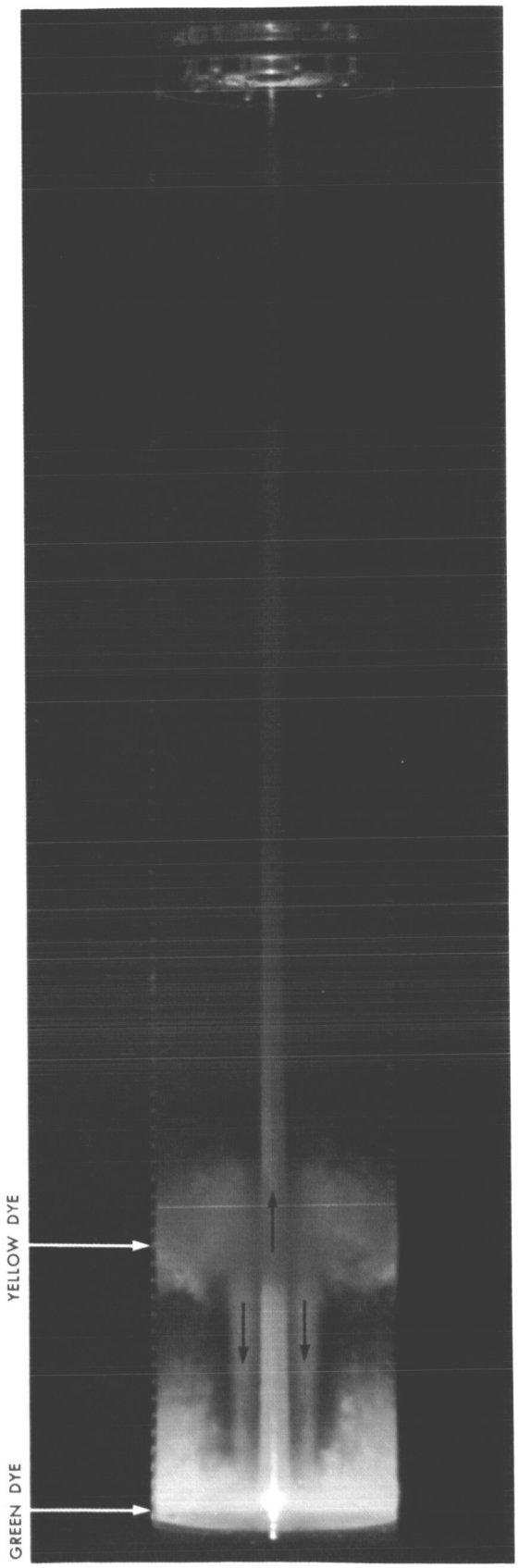

NO WIRE IN VORTEX

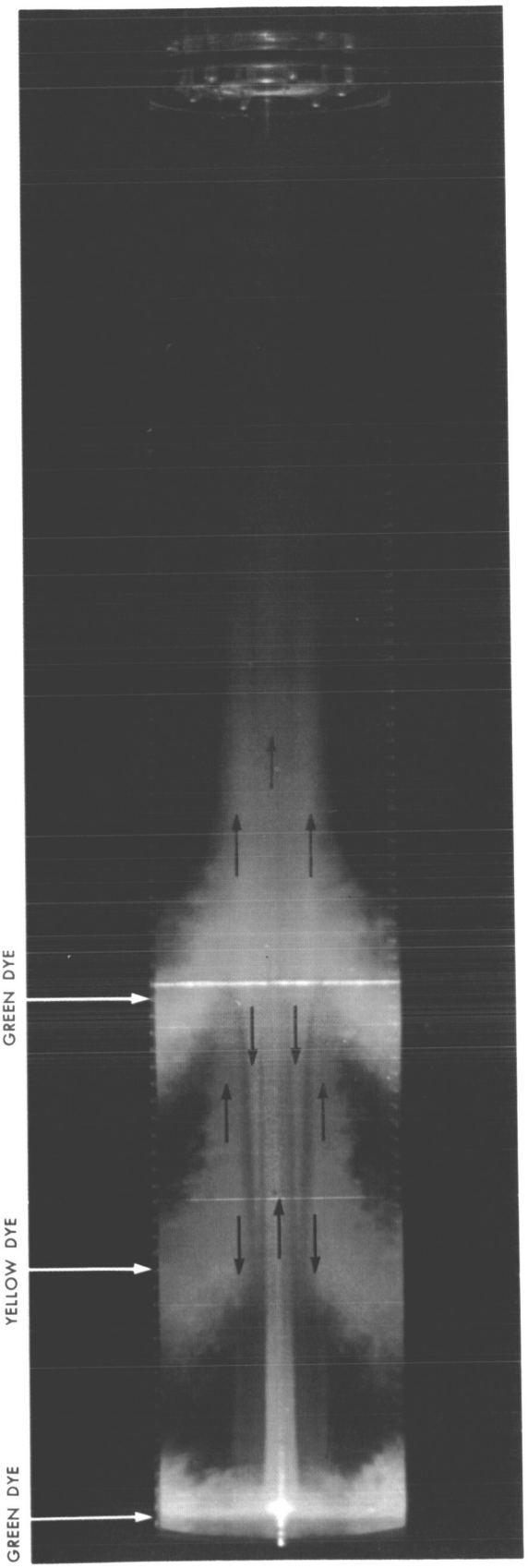

0.005-in.-diam WIRE

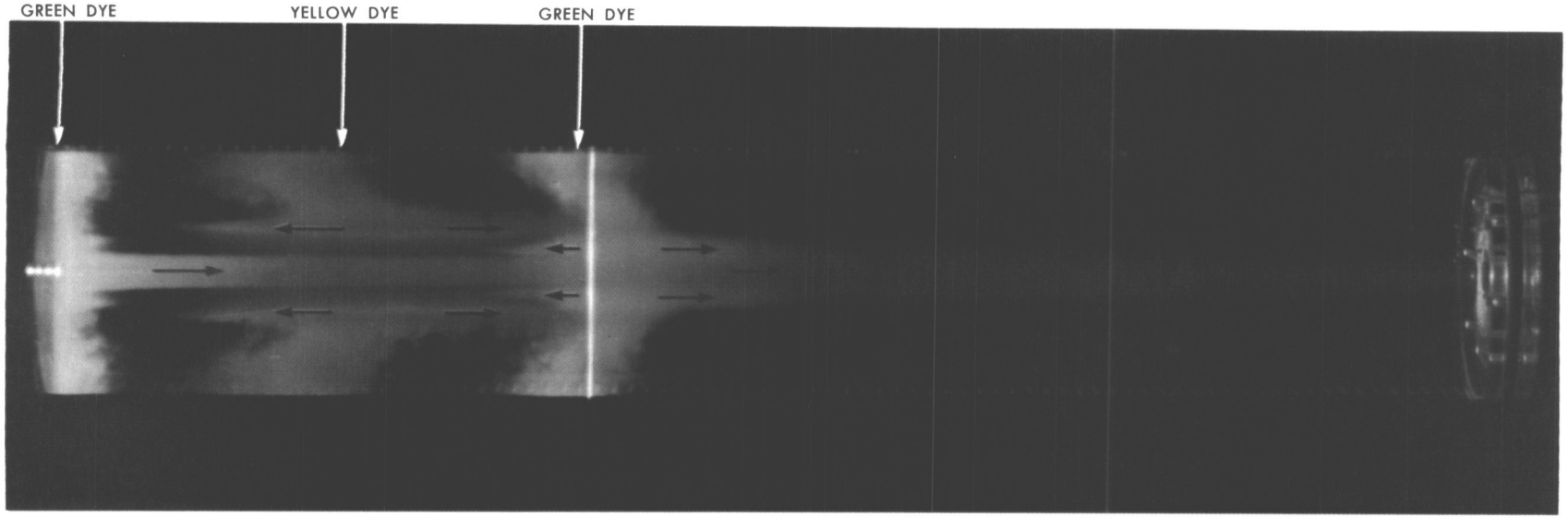

0.018-in.-diam WIRE

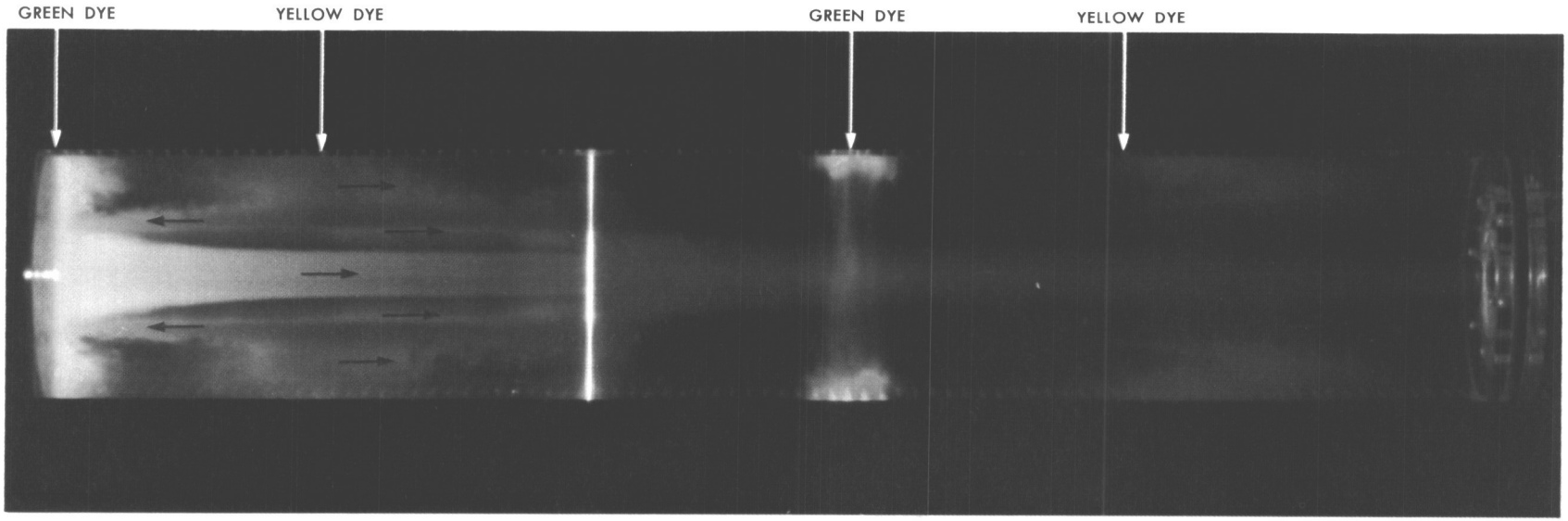

0.050-in.-diam WIRE

Fig. 11. Dye studies in standard configuration: Effect of various-size-diameter probe wires stretched across a vortex diameter, at $L/D = 5.33$ and $p_w - p_a = 5$ psig with nominal 9/10-in. exit hole

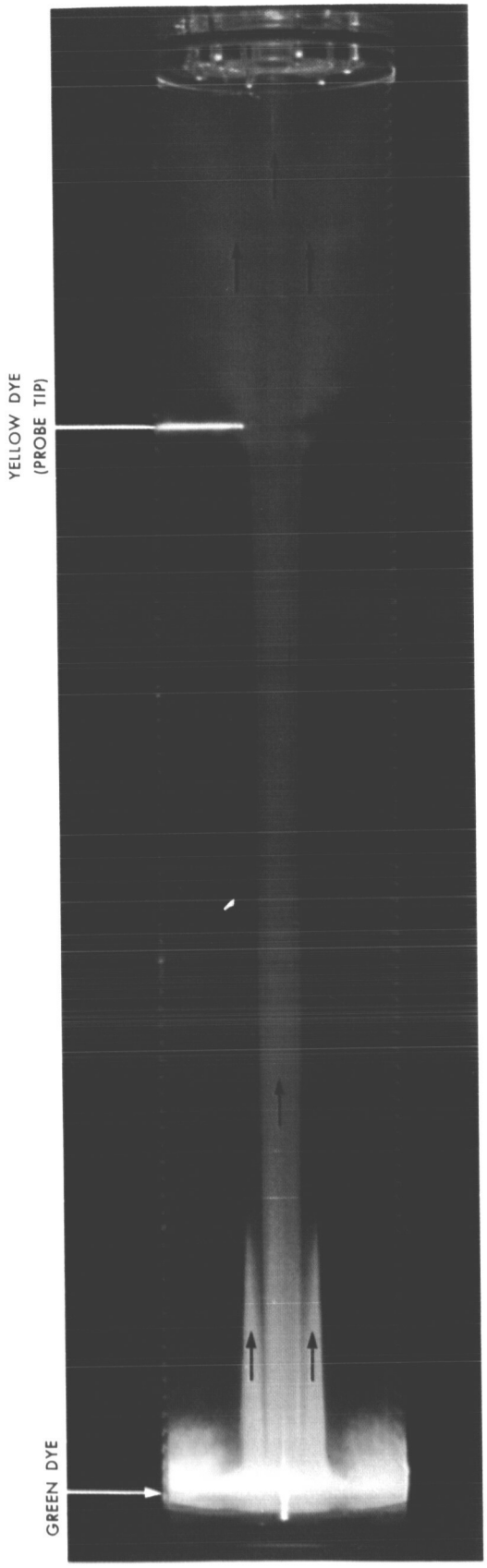

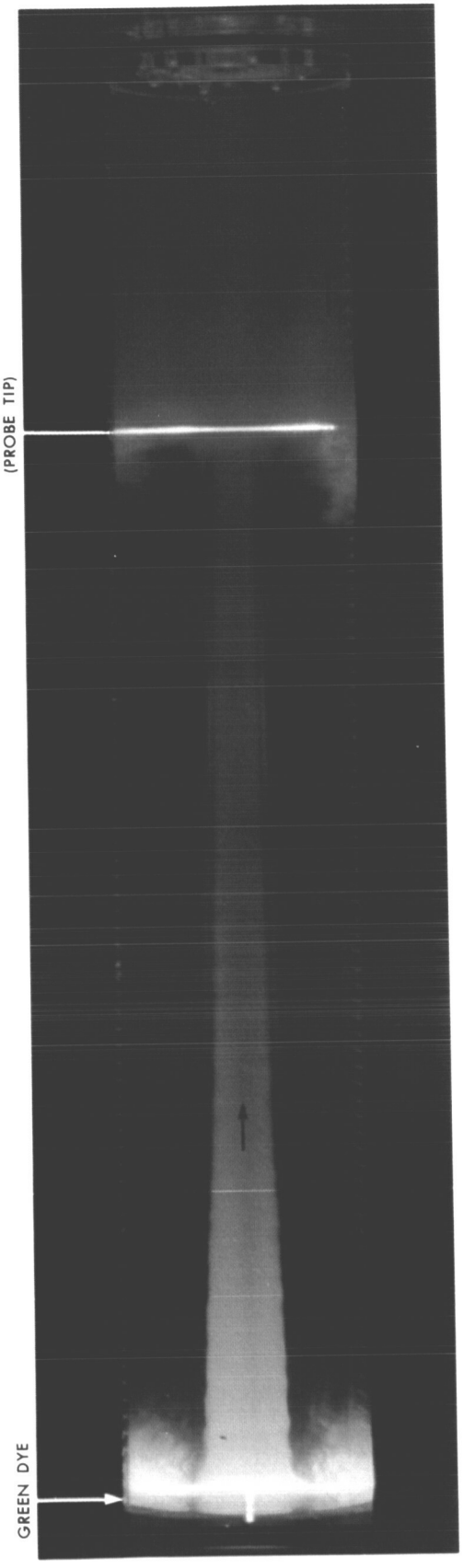

Fig. 12. Dye studies in standard configuration: Effect of cantilever-mounted probes, at $L/D = 5.33$ with nominal 9/16-in. exit hole

reveals a sharp, strong counterflow region. Further insertion of the probe so that its tip nearly touched the opposite side of the vortex tube (second photograph) again resulted in an axial counterflow and a much enlarged center jet. Endwall pressure measurements made in the cantilever-probe experiments indicated that disturbances to the flow depended on depth of penetration as well as physical probe size. Flow visualization did not reveal any significant changes in secondary flows until the probe had been inserted a half inch or more into the flow. It should be emphasized that cantilever probes, aside from their tendency to vibrate, produce disturbances decidedly less symmetric than those produced by probe wires, which also have the advantage of producing changes in vortex strength that are independent of $\dot{m}$ and axial location.

3. Miscellaneous Experiments

In this Section the results of two additional experiments will be discussed on the basis of visual observations and records by motion picture photography: (1) the effects produced by injection of a second, heavier-than-water trace fluid and (2) the effects produced by time-dependent variations deliberately introduced into the flow supply.

Carbon tetrachloride (specific gravity approximately 1.6) was introduced into the water vortex by means of injection under pressure through a small tube inserted through the cylindrical wall (Fig. 3) to the center of the vortex tube. Carbon tetrachloride and water are not miscible and the procedure just described became necessary because carbon tetrachloride injected at or near the cylindrical wall broke into rather large globules that did not migrate inward, but remained in the vicinity of the wall. This, of course, was a centrifuging effect caused by the specific-gravity difference between the two fields. Carbon tetrachloride injected near the center of the vortex was not readily swept out of the vortex in the center jet. Instead, it migrated radially outward to some equilibrium position and spread axially over a distance of several L/D to form an ill-defined, cylindrical, but annular cloud of fluid. This cloud, actually composed of numerous minute droplets, was always unstable. Wave motions developed within it, which apparently first caused breakdown into several, shorter axial segments and then radial disintegration of the various segments. During this process puffs of the heavier fluid were observed to move swiftly out of the vortex in the axial direction. Shortly thereafter, the cloud would form again at a reduced concentration, exist briefly, then disintegrate again. This cycle, not precisely periodic, would repeat many times until after many minutes very little of the original carbon tetrachloride remained. The type of instability observed in this case is probably related to unstable density stratification in the atmosphere or the sea. Instabilities of this type were the subject of a well-known paper by Synge (Ref. 20).

Incompressible rotating flows are stable or unstable according to whether the radial gradient of angular momentum (or circulation) is positive or negative (Ref. 20). One method of studying the gross effects of changes in sign of this gradient is through visualization applied to sudden changes in static pressure at the cylindrical wall brought about by changes in the rate of supply of mass flow. Modifications to the vortex apparatus were made so that sudden increases, sudden decreases, or oscillations in the static pressure at the cylindrical wall could be initiated. This was arranged by placing an adjustable time-control on the pressure in the gas-loaded dome of a regulator controlling the water flow to the vortex. Although this system was somewhat sluggish and did not produce step changes in pressure, it was adequate for the purpose. The initial rise or decay time of pressure pulses produced in this manner was fairly rapid, but it then followed a rather slow approach to the new equilibrium pressure level. Within limits, an arbitrary increment of pressure change could be effected over the entire operational range of the vortex. Oscillatory flow was established with considerably less freedom because the amplitude of the pressure pulse was found to be a strong function of frequency. However, this limitation was not crucial since visualization of oscillation frequencies much greater than approximately one cycle per second proved impossible. Pressure pulses of the order of 5 psi and oscillations of the order of 3 to 5 psi amplitude at a fraction of a cycle per second were most satisfactorily observed. The experimental procedure was to inject dye into a steady state of flow, start the motion picture camera, initiate the disturbance, and record the time-transient dye motion photographically.

The results were striking and extremely interesting; interpretations were made complicated, however, because significant changes in radial flow accompanied whatever changes in angular momentum distribution were produced. Classic mathematical stability investigations generally apply to perturbations imposed on a steady flow that does not initially possess a radial component of flow (or viscosity). Sudden increases in wall pressure were observed to produce marked stratification of the flow; dye filaments were quickly drawn out axially to form a series of nested dye cylinders, which subsequently became funnel-shaped with the end of larger diameter directed towards the closed endwall. The series of nested dye

surfaces decreased in diameter rapidly and became more drawn-out axially as both radial and axial components of flow increased significantly. The residual dye rapidly disappeared in the form of a long, slender funnel. Flows that initially appeared turbulent in the annular region became well-ordered and did not appear turbulent during this transient process. Sudden decreases in wall pressure, on the other hand, produced much different results. Dye formations initially present in the steady flow were again drawn out axially, but disintegrated radially, giving the impression of increased turbulence and increased mixing. Very rapidly, the entire vortex tube filled with a diffuse dye mixture so that individual dye colors or patterns were no longer discernible. Large radial outflows would, of course, be present in this case. In fact, initially, a significant decrease in wall pressure would cause reverse flow from the vortex back through the driving-jet orifices into the plenum chamber. Oscillations in wall pressure produced periodic transitions between the two types of flow just described. However, the process of transition from stratification to disintegration could be observed for only a few cycles until the dye became too diffuse to enable detection of individual motions.

4. Double-Exit Configuration

In modifying the vortex apparatus to a double-exit configuration (configuration B, Fig. 5) it was realized that all possible care was to be exercised in an attempt to produce symmetric or similar conditions in the two-exit-hole arrangements. Two circular exit-hole orifices $\frac{3}{8}$ in. in diameter by $\frac{9}{16}$ in. long, with rounded inlets, were centrally placed in each endwall of the vortex tube. The exit-hole orifice on one end was followed by an exit tube measuring nominally $\frac{1}{2}$ in. ID by $\frac{11}{16}$ in. OD by 8 ft long, which in turn was followed by a suitable length of flexible plastic tubing measuring $\frac{11}{16}$ in. ID. The opposite exit hole was provided with a similar exit tube that was only 2 ft long; this discrepancy in length was compensated for by increasing the length of plastic tubing on this end by an amount necessary to equal the number of pipe diameters at the opposite end. In addition, adjustable clamps were placed on both of the terminal plastic tubes so that mass rates of flow through the exit holes could be matched if the need arose.

Flow-visualization studies in this configuration were not wholly satisfactory, because the flow patterns revealed by the motion of dye injected at the midpoint of the vortex tube were far from symmetric relative to the midpoint. When adjustments were made so that the mass rate of flow through the two exit holes agreed within 5%, dye injected at any point in the vortex tube showed a clear preference to migrate toward one of the exit holes. This preference did not change, regardless of the values of total $\dot{m}$ or L/D employed; preference was always for the same exit hole. Significant reductions in mass rate of flow through the preferred exit hole did not produce a change in preference for dye extraction until the mass flow rate through that exit hole was perhaps 10% of the total mass rate of flow. Symmetry in the dye patterns was never achieved, regardless of how the total $\dot{m}$ was subdivided. Further experiments were undertaken to determine whether a mirror symmetry in secondary-flow patterns would occur if the total flow was extracted from one exit hole alone, compared to the total flow being extracted through the opposite exit hole alone. Mirror symmetry did not occur. Thus it was concluded that the exact size, shape, and location of an exit-hole arrangement must be very important in determining the exit boundary conditions of a confined vortex flow.

Other features of the flow in this configuration may be summarized as follows: (1) the secondary axial flows and counterflows appeared significantly different from those in a single-exit-hole configuration; (2) the air-core and central-jet diameters were relatively larger in the double-exit configuration than in the single-exit; (3) the flow was more often than not unsteady and seemed to display radial instabilities, which promoted increased turbulence and radial mixing since (4) dye patterns did not generally remain intact for more than a few seconds at a time. Double-exit configurations having unequal-diameter exit holes were not examined.

B. Configurations With Nonplanar Endwalls

The sketches shown in Fig. 13, 14, and 15 represent attempts to portray secondary-flow patterns in configurations C through J (Fig. 5) based on impressions gained from motion pictures. These results apply to low aspect ratio, $2 < L/D < 4$. With the exception of the diagram pertaining to configuration G in Fig. 14, air cores have been omitted from the sketches. The center jet originating at the closed endwall, which in most cases has been represented by a sharply defined region of smaller diameter than the exit hole, is not be be confused with an air core. In general, the secondary-flow patterns observed in configurations with nonplanar endwalls were more complex than in the planar configurations and also appeared to be more sensitive to changes in mass rate of flow. Cross-hatched areas in the diagrams in Fig. 13 and 14 indicate "stagnant" regions; i.e., regions that remained relatively clear and were not readily penetrated by dye except by diffusion. In time these regions

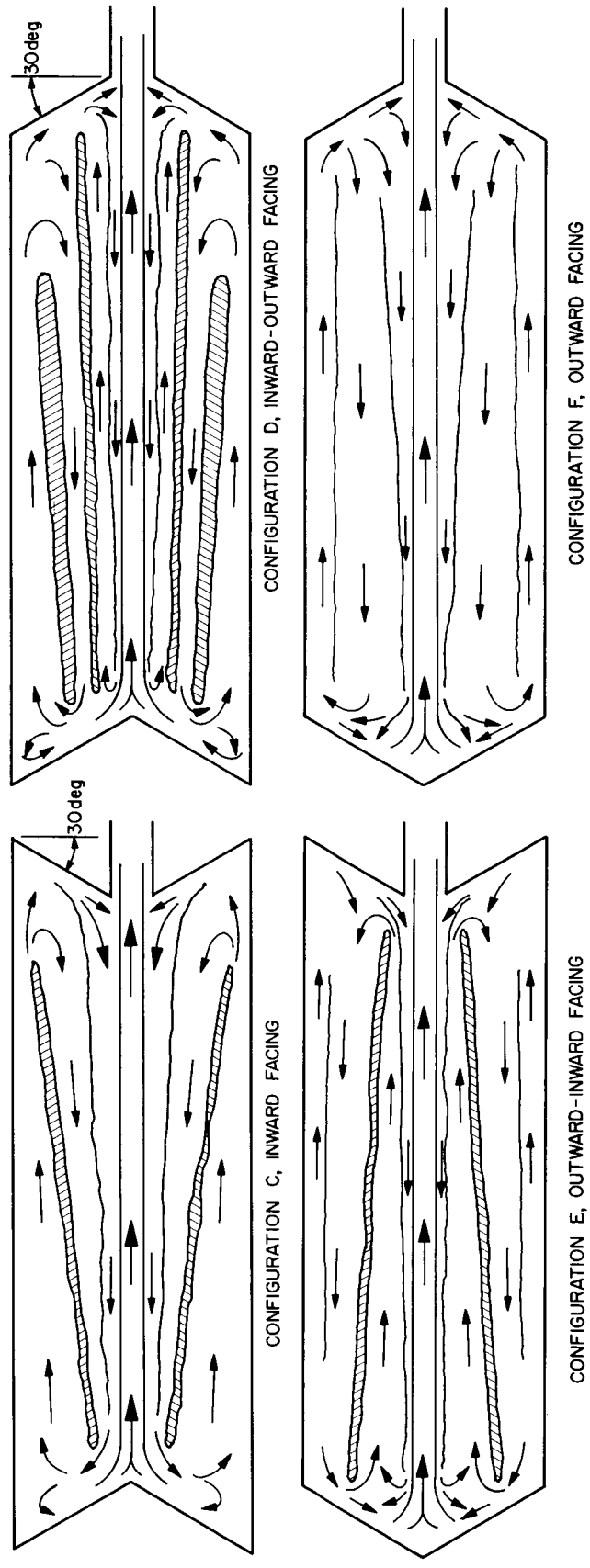

Fig. 13. Approximate secondary-flow patterns at low aspect ratio with conical endwalls; cross-hatched areas indicate stagnant regions

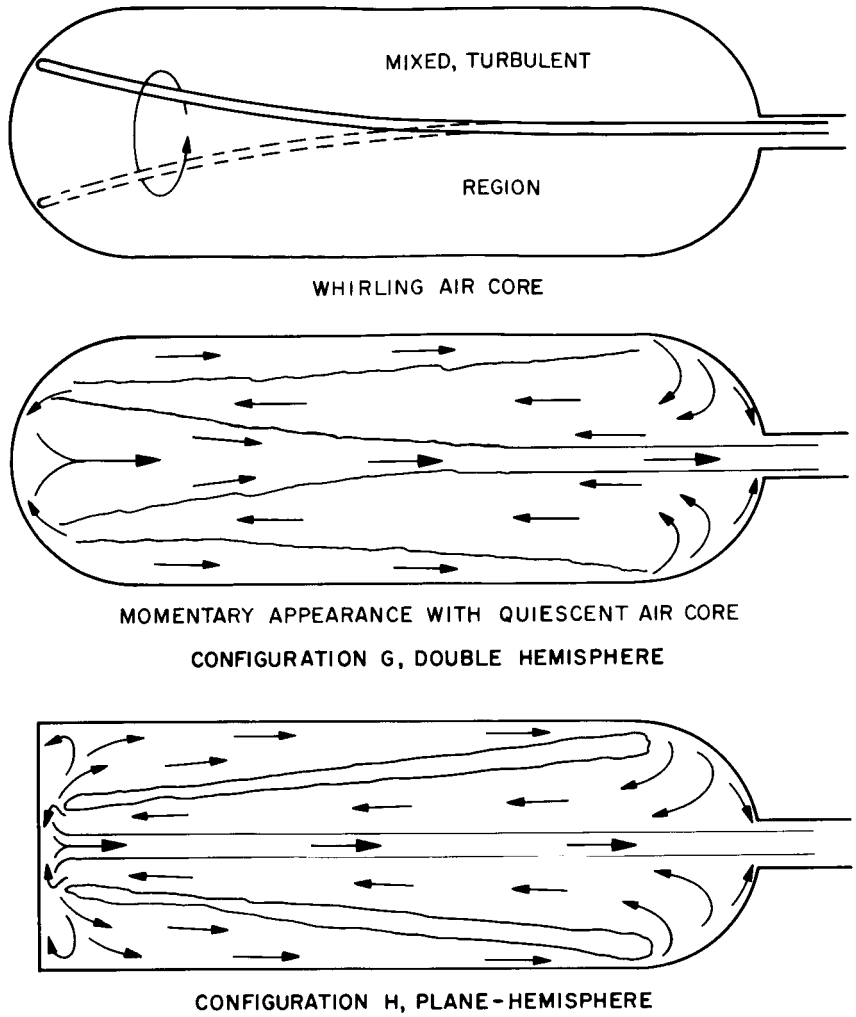

Fig. 14. Approximate secondary-flow patterns at low aspect ratio with hemispherical endwalls; cross-hatched areas indicate stagnant regions

also contained dye, which tended to be retained longer than in the remaining regions. The length, thickness, inclination, and shape of the stagnant regions were significantly influenced by both aspect ratio and mass rate of flow.

1. Conical Endwalls

Figure 13 indicates some results obtained with various combinations of conical endwalls. Flow patterns in these configurations were characterized by very strong axial flows that were not confined to thin, annular regions concentric to the central jet. Radial flows adjacent to the endwalls were also pronounced, particularly for inward-facing conical endwalls. Because of limited visibility and distortion, flow details in the apex region of outward-facing walls were not well determined.

The outstanding flow feature in configuration C (Fig. 13) was an extremely strong axial counterflow concentric to the center jet. The edge of this counterflow appeared somewhat fuzzy, especially near the right-hand endwall. Impingement on the apex of the closed endwall produced pronounced radial outflow. Secondary flows were not difficult to determine, but became more poorly determined as aspect ratio and mass rate of flow were increased. The tapered stagnant region became thinner and increasingly more cylindrical at large L/D. Mass rate of flow was recorded for configuration C and the results are plotted in Fig. 16 and 17 and compared to the results with planar endwalls reported in Ref. 1. The reduction in mass rate of flow per unit length imposed by the conical endwalls was not commensurate with their greater surface area as compared to the planar endwalls. Total endwall surface area for configuration C was

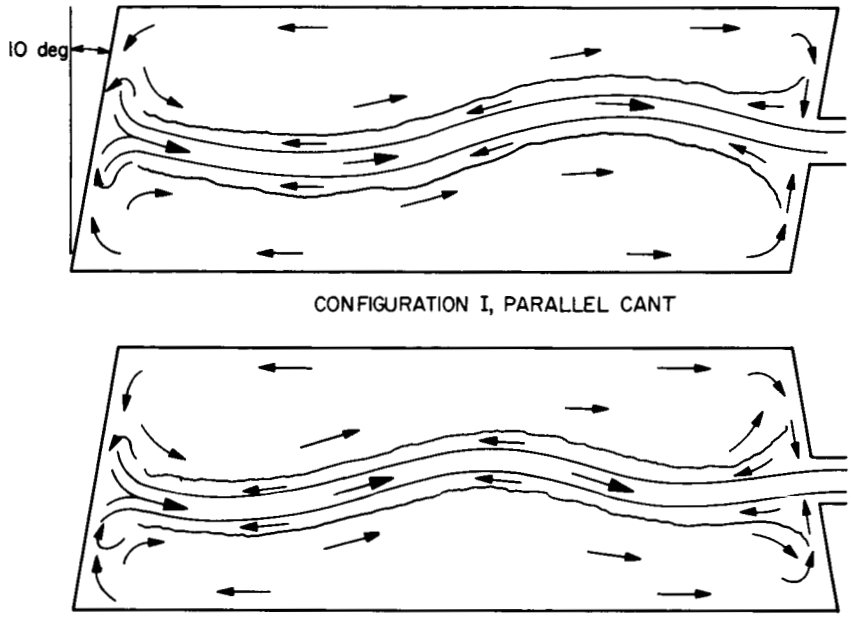

Fig. 15. Approximate secondary-flow patterns at low aspect ratio with canted endwalls

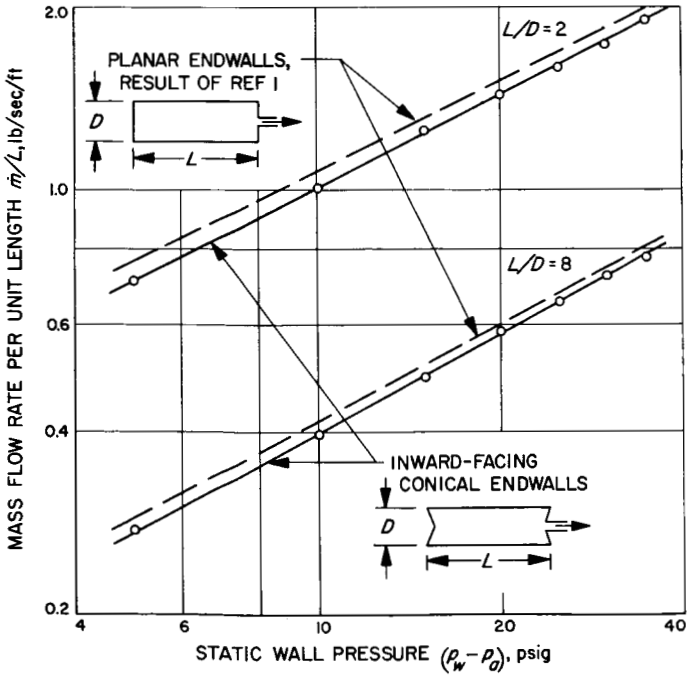

Fig. 16. Reduction in mass rate of flow per unit length due to conical endwalls; 0.498-in.-diam. exit hole

approximately 14% greater than for the planar configuration; whereas mass-flow-rate reductions were more of the order of 5%. Figure 18 contains the results of vortex-pressure difference for the two configurations at one value of wall pressure p_w. Center pressure in configuration C was measured by a tap located at the apex of the conical surface forming the closed endwall. Surprisingly, considerably lower values of center pressure were achieved with conical endwalls than with planar endwalls at $L/D < 8$.

Configuration D (Fig. 13) had the most complex flow patterns, which were perhaps the most interesting of those observed in the conical configurations. Even though the dye patterns were quite stable and well-behaved, especially at lower values of L/D, the overall picture was not readily determined because of its complexity. The innermost axial counterflow was not particularly strong in this configuration.

The innermost axial counterflow displayed by configuration E (Fig. 13) was also rather weak, but was surrounded by an axial-flow region of high strength, which produced pronounced radial outflow near the right-hand endwall. A strong axial counterflow existed near the cylindrical wall. Secondary-flow structures in configuration E appeared particularly dependent on mass rate of flow, even at low values of L/D, and the flow tended to become increasingly unsteady at high values of mass flow rate.

Secondary-flow patterns in configuration F (Fig. 13) were somewhat difficult to identify because they were ill-

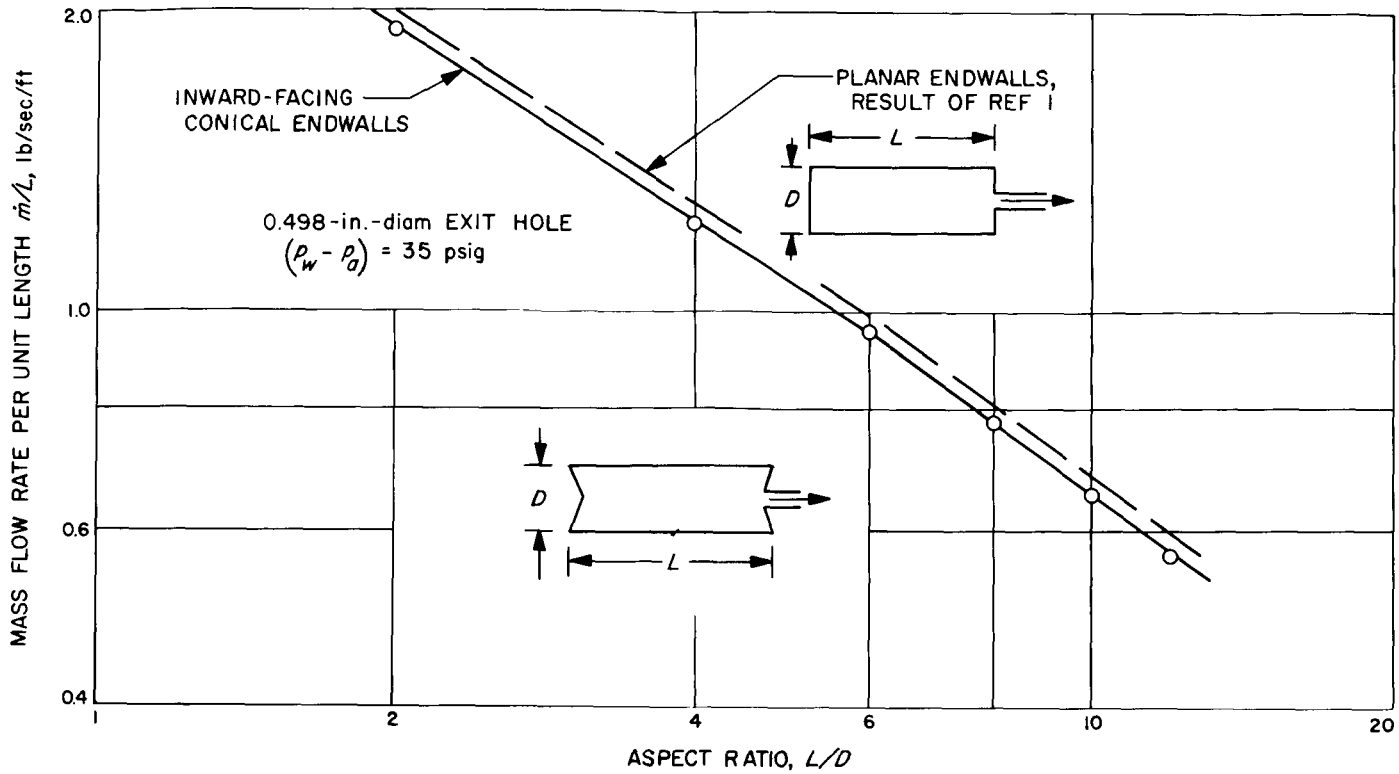

Fig. 17. Reduction in mass rate of flow per unit length due to conical endwalls

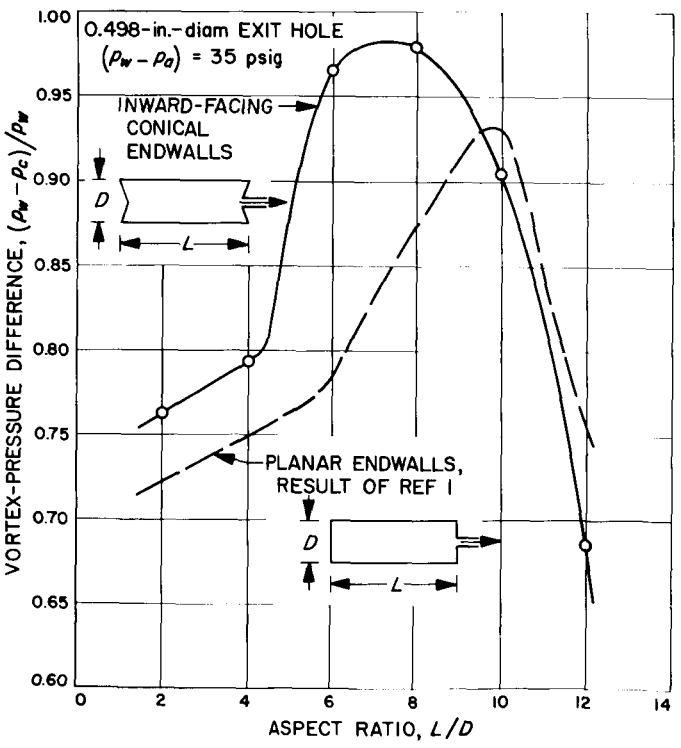

Fig. 18. Vortex-pressure difference; comparison of results obtained with conical and planar endwalls

defined, and the flow in general appeared turbulent and diffuse. Prominent axial counterflow existed relatively near the cylindrical wall. Flow in the conical apex regions could not be visualized clearly. From a visualization standpoint, configuration F was the least interesting of the conical configurations.

2. Hemispherical Endwalls

The principal feature of the double-hemisphere vortex, configuration G, was displayed by its whirling air core, as shown in Fig. 14. Axisymmetric flow in this configuration was always unstable and did not exist for more than a few seconds at a time before degeneration into the whirling mode. It is possible that this phenomenon was associated with unsymmetric boundary-layer separation on the closed endwall, which in turn may have been introduced by some slight asymmetry in surface curvature or roughness. The amplitude and frequency of the whirling air core was highly erratic, never quasi-steady, and occasionally violent. Rotation was always in the same direction as the overall flow. At times the tip of the air core moved radially outward as far as the cylindrical wall. This flow unsteadiness of course precluded effective flow visualization, since dye injected during whirling motions

rapidly diffused and mixed. Occasionally the air core would cease its whirling motion for a few seconds. Flow patterns observed in these brief interludes appeared somewhat as shown in Fig. 14, center sketch. The best that can be said for this configuration is that it was a very effective mixer. Increase of the vortex aspect ratio to larger values of aspect ratio, $L/D = 10$ or 12, did not eliminate the whirling motion. In this case a segment of the air core near the closed endwall, perhaps two or three L/D in length, exhibited erratic but interesting gyrations, whereas the remainder of the air core continued colinear with the vortex axis. The visual effect produced by the air core was similar to that produced by the whirling portion of rope attached to a spinning lariat.

Replacement of the closed, hemispherical endwall with a planar endwall (configuration H in Fig. 14) eliminated the whirling air core. The secondary-flow patterns in configuration H bore a great resemblance to those observed in configuration C (Fig. 13) at low L/D. However, the flow was less steady in configuration H and exhibited semiperiodic pulsations, which caused the boundaries of dye and stagnant regions to erratically increase and diminish in diameter.

3. Canted Endwalls

Studies of results with canted endwalls were pursued to determine the effects of large asymmetries of this type on secondary-flow structure, as a clue to the possible effects produced by smaller, unintentional asymmetries introduced by incorrect endwall alignment. In a water vortex, flow asymmetries are readily detected by misalignment of the air core with respect to the vortex-tube axis. Crooked or bent air cores, when they occur, become particularly effective indicators of flow asymmetry when they are small in diameter relative to the vortex diameter, and the vortex aspect ratio is relatively large. Flow asymmetries may arise in many ways: (1) asymmetric fluid injection or injection at too few locations, such as occurs in most cyclone separators, (2) out-of-round cylindrical wall, (3) misaligned endwalls, (4) misaligned and/or eccentric exit holes, and (5) introduction of probes, particularly cantilever-mounted probes.

As expected, canted endwalls produced highly asymmetric flows characterized by sinuous core regions (Fig. 15). In the parallel-cant configuration I, the terminal regions of the core flow appeared roughly perpendicular to the endwalls. End-view sightings along the undulating core and center jet indicated that they were sinuous in a vertical plane, i.e., the plane of the paper, and not spiral-shaped. Variations in wavelength did not appear to be large over a large range of flow conditions, so that the steadiness of the sinuous-core flow depended somewhat on the aspect ratio of the vortex tube. Unsteadiness became manifest by perturbations traveling axially along the center jet or general oscillations of the wave in the vertical plane. A standing wave, steady in time, was relatively easy to produce over a wide variety of flow conditions and aspect ratios.

Compared with configuration I, configuration J (Fig. 15) exhibited considerably more flow unsteadiness. Configuration J was produced merely by rotating the piston (Fig. 1) 180 deg. The plane of the core flow, predominantly sinuous but now with a slight spiral or corkscrew effect, appeared to shift approximately 45 deg out of the vertical plane. The wavelength appeared to be more definite in this case and was estimated to be approximately four L/D. Figure 15, being schematic, is somewhat distorted. Standing waves were much more difficult to produce and maintain in configuration J than in configuration I, and slight variations in L/D were sufficient to cause onset of unsteadiness. It was also noted that the origin of the center jet at the closed endwall always fell considerably below the center point of that endwall (Fig. 15). The dye patterns produced in both configurations with canted endwalls were striking and beautiful when the core wave was stationary in time.

C. Configurations With Submerged Exit Tubes

Configurations K and L (Fig. 5 and 19) were investigated on the premise that an increase in the resistance to flow in the endwall boundary layers might reduce the flow therein, and thereby result in a relatively larger radial inflow away from the endwalls. The increased resistance was produced by submerging or inserting the exit tubes into the vortex flow, thus increasing the fluid path length of flow entrained in the endwall boundary layers. It was realized that any increase in radial inflow would be virtually impossible to detect by visual means; however, the secondary-flow patterns in these configurations were of some interest. Aspect ratio and depth of submergence of the exit tubes were both variable in these experiments. The general effect of submerged exit tubes was judged to be detrimental; separated flow regions generated in the corners of the vortex tube adjacent to the exit tubes gave rise to a turbulent, confused flow and a reduction in vortex strength as compared to effects with exit tubes extracted flush with the endwalls. Strong axial flows and counterflows developed in configurations K and L.

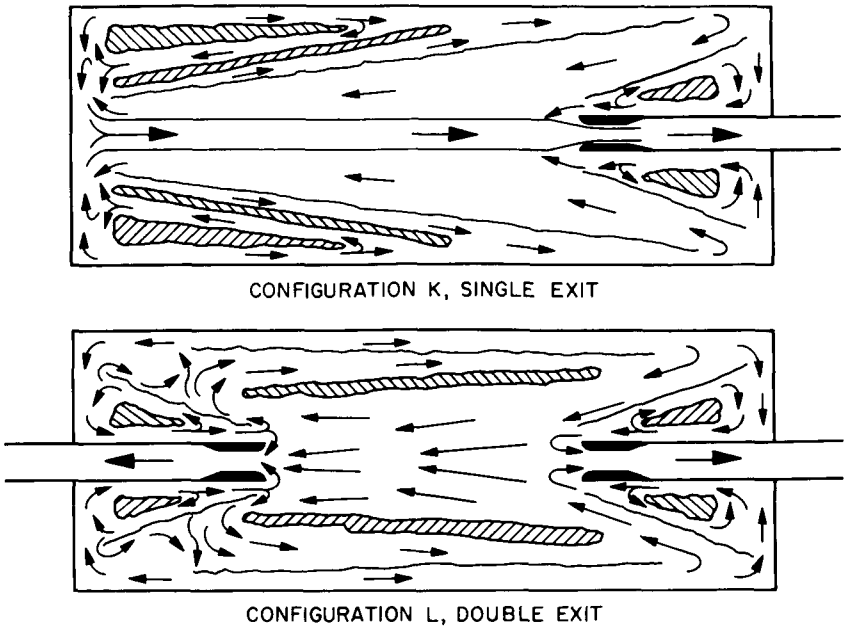

Fig. 19. Approximate secondary-flow patterns at low aspect ratio with submerged exit tubes; cross-hatched areas indicate stagnant regions

One feature noted with the single submerged exit tube, configuration K, was a center jet that was generally larger in diameter than the exit-hole orifice. Just prior to exhaust, the center jet necked down to form a vena contracta. Flow in configuration L was extremely difficult to determine. This was due to very rapid axial motions, rapid dye diffusion, and poor lighting conditions. Since light was admitted through the left-hand endwall at an angle to the vortex axis, shadows produced by the exit tubes obscured detail in the core region between the exit-hole orifices. Just as in configuration B (Section IV-A4), flow symmetry could not be achieved and dye extraction from the vortex showed a decided preference for the left-hand exit tube.

V. DISCUSSION

When interpreting the results of flow-visualization studies, one is immediately confronted with the necessity of differentiating between fluid-stream lines, particle-path lines, and streak or filament lines. When the flow is steady these three motions are identical (Ref. 21 and 22). However, when the flow is unsteady in time the motions are different to an extent determined by the flow field and the degree or nature of the unsteadiness. If, in addition to the kinematics of fluid particles, trace particles differing in density with the surrounding fluid are utilized, other body forces due to buoyancy, inertia, etc., must be considered; initial conditions must be taken into account. Treatment of the last problem for steady fluid flows is given in Ref. 23, including application to rotating flows. In the present study, the density-difference problem was considered to be of negligible importance, since water-soluble dye solutions were used as trace or marking fluids. Injection of dye in water or smoke in air viewed at a later instant in time yields the so-called streak or filament line; i.e., a line joining the positions of all particles that have previously passed through a designated point in space, at some particular instant of time. Reference 24 provides a good illustration of existing pitfalls that can easily lead to misinterpretation of dye motions. In Ref. 24 the behavior of streaklines in a sinusoidally perturbed shear flow was investigated, a phenomenon important to the

study of boundary-layer transition. Streaklines in such a flow were found to roll up, giving an impression that discrete vortices were being formed despite the fact that the initial disturbance was not amplified. This result may have bearing on the present studies in a vortex flow, which, of course, is another special case of shear flow.

The vortex flows studied here were steady for the most part, although perhaps turbulent. Many cases of unsteadiness did arise, however. Because of the general flow steadiness and because detailed streamline pictures were not required, no special consideration was given to interpretations as might be modified by a time-varying flow, except in the instances noted. Nevertheless, many interpretative problems do exist for flows of this type, some of which will be discussed presently.

The designations "laminar" and/or "turbulent" used in this Report may be considered by some as pure speculations, being based solely on the appearances of dye filaments. It is certainly true that the human eye or a camera operating at normal frame rates has limited capacity for resolving frequency and amplitude. For example, a high-frequency, low-amplitude fluctuation might go completely undetected. However, within its frequency-detection range, the eye is a reasonably good detector of randomness, unless the observed waveform is very complex but nevertheless periodic. When viewed from the side, vortex flows designated as turbulent appeared to have large, local, random fluctuations. Here again one can be misled. Consider a ring-shaped dye filament bearing slight eccentricity or a local "bump" rotating within an otherwise laminar fluid. Viewed edge-on, the appearance and disappearance of the bump would give the impression of a radial but periodic fluctuation. However, an array or formation of such rings traveling axially might give the impression of turbulence. Such a case is not likely to occur often, so it is doubtful one could be fooled for long, especially when utilizing end views in addition to side views. It is believed that flows described as turbulent were in fact turbulent. The same statement applied to laminar flows is made with less assurance. Another consideration involved in judgments of the nature of the flow was the rate of dye diffusion, which was considerably greater when so-called turbulence was present. Motion pictures made at rates of 128 frames/sec did not seem to differ from those made at 24 frames/sec.

The internal structure of flow within thin shear regions, e.g., axial flows and counterflows, could not be determined by these visual experiments. That is, one could not tell whether the advance of a dye front in the form of a thin annular cylinder progressing axially represented a general axial flow along the annular layer or whether the streamlines folded at the face of the front, hence bearing fluid back to the boundary layer from which it originated. Examples of the latter situation are contained in Ref. 25. Axial flows and counterflows shown in the photographs and schematic flow diagrams of this Report are simply indicated by arrows that designate the overall direction of motion of the dye front.

Edge-on views of inward-facing conical surfaces produced a phenomenon, or perhaps an impression, worth describing. Dye injected near the base of the conical surface first appeared to move in very rapidly to the apex and then a portion of the dye appeared to move radially outward almost as rapidly. This was taken as a good indication of radial outflow just outside the boundary layer on these conical surfaces. The notion that this event may have been partly illusory may be appreciated by reasoning as follows. Dye within the boundary layer, having a high radial component of velocity, would move in to the apex rapidly, whereas dye near the edge of the boundary layer would proceed in the radial direction more slowly. This timing difference could give rise to a barber-pole effect leading to the impression of an outward flow where none existed. Similar comments would apply to the apparent direction of helical dye filaments, because the rotation of a helix gives the impression of axial motion.

Worthy of comment is another possible false conclusion that might be derived from observing stable-appearing dye cylinders. One might infer that zero radial flow occurred across these regions, since radial flow would disturb the integrity of the dye cylinder. However, radial-velocity components in a vortex flow are so small compared to the tangential components that such motions could not be discerned. Dye cylinders originating at one endwall do not always extend fully to the opposite endwall and yet the dye disappears somewhat more rapidly than would be expected by diffusion alone.

In Ref. 1 statements were made concerning the effect of small air cores on the radial distribution of pressure at the closed endwall. It was concluded that the presence of very small air cores did not greatly affect the readings taken and probably did not affect the vortex flow significantly. However, it must be realized that an air core does affect the flow in at least three ways: (1) It modifies the terminal boundary conditions on the endwall boundary

layers; (2) it effectively prevents any radial flow of water within its bounds and hence may modify the core flow; and (3) it serves as a restriction within the exit hole by reducing the discharge area. The sum total of these effects is unknown and undoubtedly depends on the relative size of the air core, which, in Ref. 1, was found to depend strongly on exit-hole size and aspect ratio, but was not greatly affected by mass rate of flow. It should be repeated here that the occurrence of air cores in these experiments was not due to atmospheric recirculation in the subatmospheric-pressure region of the vortex, but rather to gas coming out of solution from the water itself.

VI. SUMMARY AND CONCLUSIONS

Visual observations of the flow of water within a confined, jet-driven vortex tube have been presented and described. These observations were accomplished by means of dye injections into the same apparatus used in Ref. 1; the principal visual features observed in the various configurations are summarized in Table 1. Results obtained using configurations with planar endwalls clearly showed (1) the highly three-dimensional nature of vortex flows of this type and (2) the strong influence of aspect ratio L/D on such flows, especially at lower values of L/D, which are dominated by endwall boundary layers and their interactions with the primary vortex flow. One such effect is the variation in area over which axial discharge from these boundary layers occurs. In general, the effect of increasing L/D is to decrease the vortex-core diameter. Secondary-flow patterns were not significantly affected by changes in mass rate of flow $\dot{m}$ at low values of L/D. However, at larger values of L/D, significant effects produced by changes in $\dot{m}$ were sometimes observed. Turbulence appeared to increase both with L/D and $\dot{m}$, except in the core region of the flow where no turbulence was evident. Insertion of probes into the flow was found to have significant effects on the secondary-flow patterns.

Results obtained with nonplanar endwalls (conical, hemispherical, and canted) indicated an increase in both axial and radial secondary flows as compared with results obtained with planar endwalls. In general, secondary flows were less confined to the core region and occupied a larger radial domain in configurations with nonplanar endwalls.

NOMENCLATURE

d_e diameter of exit hole
D diameter of vortex tube
L length of vortex tube
$\dot{m}$ mass rate of flow
p_w static pressure at the cylindrical wall, absolute
p_c static pressure at vortex center (measured at endwall), absolute
p_a atmospheric pressure

REFERENCES

1. Roschke, E. J., *Experimental Investigations of a Confined, Jet-Driven Water Vortex,* Technical Report No. 32-982, Jet Propulsion Laboratory, Pasadena, Calif., October 1, 1966.

2. Ross, D. H., *An Experimental Study of Secondary Flow in Jet-Driven Vortex Chambers,* Aerospace Corp., El Segundo, Calif., Report No. ATN-64 (9227)-1, January 1964.

3. Rosenzweig, M. L., Ross, D. H., and Lewellen, W. S., "On Secondary Flows in Jet-Driven Vortex Tubes," *Journal of Aerospace Sciences,* Vol. 29, No. 9, September 1962, pp. 1142, 1143.

4. Kendall, J. M., *Experimental Study of a Compressible Viscous Vortex,* Technical Report No. 32-290, Jet Propulsion Laboratory, Pasadena, Calif., June 1962.

5. Binnie, A. M., and Kamel, M. Y. M., "Experiments on the Flow of Water in a Tube at High Rates of Swirl," *Houille Blanche,* Vol. 14, No. 3, May–June 1959, pp. 348–360.

6. Keyes, J. J., Jr., "An Experimental Hydromagnetic Investigation of Jet-Driven, Confined Vortex-type Flow," in *Developments in Theoretical and Applied Mechanics,* Vol. 2 (Proceedings of the 2nd Southeastern Conference on Theoretical and Applied Mechanics, held at Georgia Institute of Technology, March 1964), Pergamon Press, New York, 1965, pp. 227–296.

7. White, A., "Flow of a Fluid in an Axially Rotating Pipe," *Journal of Mechanical Engineering Science,* Vol. 6, No. 1, January 1964, pp. 47–52.

8. Chanaud, R. C., "Observations of Oscillatory Motion in Certain Swirling Flows," *Journal of Fluid Mechanics,* Vol. 21, Part 1, January 1965, pp. 111–127.

9. Smith, J. L., Jr., "An Experimental Study of the Vortex in the Cyclone Separator," *Journal of Basic Engineering* (Transactions of the ASME, Series D), Vol. 84, 1962, pp. 1–7.

10. Astill, K. N., "Studies of the Developing Flow Between Concentric Cylinders With the Inner Cylinder Rotating," *Journal of Heat Transfer* (Transactions of the ASME, Series C), Vol. 86, 1964, pp. 383–391.

11. Magarvey, R. H., and MacLatchy, C. S., "The Formation and Structure of Vortex Rings," *Canadian Journal of Physics,* Vol. 42, April 1964, pp. 678–683.

12. Hagerty, W. W., "Use of an Optical Property of Glycerine-Water Solutions to Study Viscous Fluid-Flow Problems," *Journal of Applied Mechanics,* Vol. 17, March 1950, pp. 54–58.

13. Bunting, L. S., and Kreith, F., "Flow Visualization Method for Three-Dimensional Incompressible Fluid Flow," *Review of Scientific Instruments,* Vol. 34, No. 4, April 1963, pp. 447, 448.

14. Van Meel, D. A., and Vermij, H., "A Method for Flow Visualization and Measurement of Velocity Vectors in Three-Dimensional Flow Patterns in Water Models by Using Color Photography," *Applied Scientific Research,* Sect. A, Vol. 10, 1961, pp. 109–117.

REFERENCES (Cont'd)

15. "An Optical Technique for Measuring the Vortex Velocity of a Fluid Without Interfering With Its Flow," *Product Engineering*, Vol. 35, No. 9, April 27, 1964, p. 64.

16. Kelsall, D. F., "Study of the Motion of Solid Particles in a Hydraulic Cyclone," *Transactions of the Institute of Chemical Engineers* (London), Vol. 30, No. 2, 1952, pp. 87–104.

17. Grey, J., *A Gaseous-Core Nuclear Rocket Utilizing Hydrodynamic Containment of Fissionable Material*, ARS Paper No. 848-59, presented at the American Rocket Society Semi-Annual Meeting, San Diego, Calif., June 1959.

18. Muckenhaupt, J. E., "Visualizing Bounded Flows," *Research/Development*, Vol. 35, No. 12, December 1964, pp. 24–25.

19. Pivirotto, T. J., *An Experimental and Analytical Investigation of Concentration Ratio Distributions in a Binary Compressible Vortex Flow*, Technical Report No. 32-808, Jet Propulsion Laboratory, Pasadena, Calif., March 15, 1966.

20. Synge, J. L., "The Stability of Heterogeneous Liquids," *Transactions of the Royal Society of Canada*, Vol. 27, 1933, pp. 1–8.

21. Prandtl, L., and Tietjens, O. G., *Fundamentals of Hydro- and Aeromechanics*, Engineering Societies Monographs, Dover Publications, Inc., New York, 1957, pp. 72–77.

22. Pankhurst, R. C., and Holder, D. W., *Wind-Tunnel Technique*, Isaac Pitman and Sons, London, 1952, pp. 137–139.

23. Wright, F. H., *The Particle-Track Method of Tracing Fluid Streamlines*, Progress Report No. 3-23, Jet Propulsion Laboratory, Pasadena, Calif., March 1951.

24. Hama, F. R., "Streaklines in a Perturbed Shear Flow," *Physics of Fluids*, Vol. 5, No. 6, June 1962, pp. 644–650.

25. Anderson, O. L., *Theoretical Solutions for the Secondary Flow on the End Wall of a Vortex Tube*, Report R-2494-1, United Aircraft Corp., Research Labs., East Hartford, Conn., 1961.

APPENDIX

Selection of Dyes and Photographic Film

Information on several fluorescent dyes is given in Table A-1. Rhodamine B and dichlorofluorescein were selected on the judgment that they constituted the best overall color combination over a wide range of conditions. Uranine and fluorescein dyes seem to be quite similar in characteristics and color except, perhaps, that fluoresceins are somewhat brighter; they can probably be used interchangeably without adverse effects. The fluorescent blue dyes were not used because UV illumination was discarded in favor of "white" light, i.e., a Sun Gun. Of all the dyes tested, anionic additive proved easily the best when using black and white film and UV illumination; it also shows well on blue-sensitive color film when using UV illumination. B-Methyl umbelliferone fluoresces very well and photographs in color well; however, it cannot be used in very great concentration because it tends to precipitate. With ultraviolet light, it would be very effective for use in small apparatus using sharp, well-collimated slit illumination, since it is almost transparent to white light and does not obscure vision except where illuminated by UV.

Table A-1. General information on water-soluble, fluorescent dye powders

Dye	Natural color of powder	Solubility in water	Appearance of solution			Remarks
			UV[e]	Daylight	Sun Gun[f]	
Rhodamine B[a]	Red-black	Good	Deep orange	Pink	Orange to yellow	Somewhat difficult to mix; persistent biological stain; slowly attacks brass
Dichlorofluorescein[b]	Dark orange	Excellent	Yellow-green	Green to yellow	Green to yellow	Excellent for general purpose
Uranine[c]	Orange	Excellent	Yellow-green	Turbid yellow-green	Mostly green	Good for general purpose
B-methyl umbelliferone[a]	White	Poor	Deep blue	Almost colorless	Almost colorless	Mixes poorly and saturates readily; solution contains particles
Flux additive[d]	Pale yellow	Good	Ice blue	Almost colorless, faint brown	Gray-white	Requires large concentration for UV visualization
Anionic additive[d]	Bright yellow	Good	Blue-white	Murky white	Blue-green	Shows very well on black and white film using UV illumination

[a] Matheson Company, East Rutherford, N.J.
[b] Eastman (Kodak) Organic Chemicals, Rochester, N.Y.
[c] Fisher Scientific Company, Fairlawn, N.J.
[d] Ultraviolet Products, San Gabriel, Calif.; additive Nos. DF-545, DF-563, respectively.
[e] Long-wave ultraviolet.
[f] Mercury vapor lamp.

No special problems arose with film. For still shots Ekta S was generally used. Both Ektachrome (color positive) and Ektacolor (color negative) films were used, but the latter appeared to give sharper contrast in this application, especially when color prints were desired. Since Ektachrome is color positive it is necessary to go through an intermediate process to obtain color prints from transparencies. Those reproduced here are direct reversal prints. Figures 9, 11, and 12 were made from Ektacolor negatives and appear superior in quality to Fig. 6, 7, 8, and 10. Both Ektachrome ER (daylight) and Ektachrome ER-B (color-compensated to 3200°K) were used in making motion pictures, with little apparent difference in the results.

ACKNOWLEDGMENTS

Photography in connection with vortex visualization was undertaken by Donald Maxeiner and Robert Hansen of the Jet Propulsion Laboratory photography staff; their advice and aid was greatly appreciated. Care and modification of the apparatus was efficiently handled by William Thogmartin and Francis Slover.